2023-05-05

Characteristics of a Novel Alkali Flame Ionization Detector as an Air Sensor for Volatile Organonitrogen Compounds

Mogenson, Cole Mitchell

UNIVERSITY OF CALGARY

Characteristics of a Novel Alkali Flame Ionization Detector as an Air Sensor for Volatile Organonitrogen Compounds

by

Cole Mitchell Mogenson

A THESIS

SUBMITTED TO THE FACULTY OF GRADUATE STUDIES

IN PARTIAL FULFILMENT OF THE REQUIREMENTS FOR THE

DEGREE OF MASTER OF SCIENCE

GRADUATE PROGRAM IN CHEMISTRY

CALGARY, ALBERTA

MAY, 2023

Abstract

This thesis describes the introduction and characterization of a novel alkali flame ionization detector (AFID) for use as an air sensor for organonitrogen compounds without any chromatographic separation. Using a planar channelled quartz design, a simple, lightweight architecture for the portable device is presented, which yields a sensitive and selective response toward nitrogen-containing analytes over hydrocarbons. For instance, the AFID sensor offers a detection limit of 30 pg N/s and a selectivity for nitrogen response over carbon of nearly two orders of magnitude. Further, the nitrogen response was linear over the 1000-fold range of concentrations investigated.

Relative to a flame photometric detector (FPD) device also used in a sensor mode under optimal conditions, the AFID was observed to provide over a 160 times greater S/N value for nitrogen analytes with a selectivity of nitrogen over carbon that was about 16.6 times larger. When using the AFID and FPD sensors in tandem, it was found that the response ratio of the simultaneous signals generated by each produced characteristic signal ratio values that more clearly identified the presence or absence of nitrogen in unknown analytes.

The AFID sensor was also used to detect organonitrogen analytes in several sample matrices. Results indicate that signal response was largely unaffected by these potentially interfering sample conditions, and thus this method could be a valuable approach for portable air sensing of nitrogen compounds.

Preface

Portions of Chapter Two, Three, Four, and Five have been submitted for publication in the Canadian Journal of Chemistry as “Characteristics of a Novel Alkali Flame Ionization Detector as an Air Sensor for Volatile Organo-Nitrogen Compounds” and is currently pending approval.

Acknowledgements

First and foremost, I would like to thank my supervisor, Dr. Kevin Thurbide, for his continuous support and guidance throughout my degree. I am incredibly appreciative for the opportunity to research and learn under his supervision and am a better person and chemist because of him. I would also like to thank my supervisory committee, Dr. Susana Kimura-Hara and Dr. Max Anikovskiy, for their assistance throughout my degree, in both a learning and teaching environment.

I am also grateful for all members of the Thurbide research group, past and present. Thank you for all your ideas and help throughout my degree, as well as all the fun times we shared over the years.

I would also like to acknowledge and thank everyone in the science workshops who have lent their skills and knowledge to this project. Especially Mark Toonen, without whom the work done in this thesis would have been quite literally impossible. I also could not have done this without the many other people whom I've met or have helped me throughout my degree. Professors, chemistry support staff, fellow students, thank you for all you have imparted to me, big or small.

Finally, I would also like to thank my family as well as my partner for their encouragement and patience throughout my educational pursuits.

Table of Contents

List of Tables

List of Figures

List of Symbols, Abbreviations, and Nomenclature

ACN	acetonitrile
AFID	alkali flame ionization detector
~	approximately
b.p.	boiling point
CK	cyanogen chloride
°C	degrees Celsius
DEA	diethylamine
ECD	electron capture detector
et al.	et alia (and others)
e.g.	exempli gratia (for example)
FID	flame ionization detector
FPD	flame photometric detector
g	gram
g/mL	grams per milliliter
g X	grams of a certain element or compound
g X/s	grams of a certain element or compound per second
GC	gas chromatography

>	greater than
≥	greater than or equal to
AC	hydrogen cyanide
i.e.	id est (in other words)
IDLH	immediately dangerous to life or health
IMS	ion mobility spectroscopy
L	liter
LOD	limit of detection
MS	mass spectrometer
µg	microgram
µL	microlitre
mL/min	milliliters per minute
mm	millimetre
mV	millivolt
min	minute
ng	nanogram
ng/mL	nanogram per millilitre
NCD	nitrogen chemiluminescence detector

NPD	nitrogen-phosphorus detector
N/C	nitrogen to carbon ratio
N_{p-p}	Noise peak-to-peak
N_{rms}	noise root-mean-square
ppm	parts per million
%RSD	percent relative standard deviation
PMT	photomultiplier tube
pg	picogram
RbCl	rubidium chloride
$RbNO_3$	rubidium nitrate
Rb_2SO_4	rubidium sulfate
S/N	signal-to-noise ratio
SS	stainless steel
TCD	thermal conductivity detector
TID	thermionic emission detector
v/v	volume by volume

Chapter One: Introduction

1.1 Importance of Organonitrogen Compounds

Organonitrogen compounds are essential in a wide variety of natural and biological processes and industrial sectors, such as petroleum and pharmaceutical production.[1–5] Many airborne organonitrogen molecules are of particular interest due to their ability to easily spread and influence numerous chemical systems. For instance, one well-studied example is peroxyacetyl nitrate (PAN), a lung and eye irritant formed as a secondary pollutant in photochemical smog.[6,7] Amines, amides, alkyl nitrate/nitrites, nitrosamines and nitroarenes have also been identified and traced to several sources, including industrial emissions, fossil fuel combustion, and sewage treatment.[7] More deliberate uses of airborne organonitrogens also exist. Carbamate pesticides, for instance, have been used globally in agriculture and have provided tremendous benefits in food production. However, they are known to be neurologically and reproductively damaging to humans[8] and environmentally destructive.[9] Even more sinister is the use of chemical warfare agents. Many nerve agents of both traditional and modern designs, as well as blood agents, blister, and other sensory agents, usually contain one or more nitrogen atoms.[10] Aerosolized nervous system acting agents, like fentanyl and its derivatives, have even been thought to be used as warfare agents.[11,12]

Due to the abundance and variance of airborne organonitrogens, rapid analysis is critical in confirming the presence of these species to aid in regulatory and risk response. Unfortunately, current analytical methods available for nitrogen detection are often immobile and bench-top bound, thus increasing the testing process time, which can delay

response measures in potentially critical situations. Additionally, portable systems for in-situ testing are either not selective towards nitrogen, or if they are, are often complex and expensive systems that require several intricate components necessary for detection. As such, the need for a portable, cost-effective, and simply designed system that can be deployed in the field to give rapid feedback is a desirable asset in the realm of airborne organonitrogen detection. The focus of the work involved in this thesis will be the development of such a system for in-situ, rapid, nitrogen-selective detection while remaining lightweight, portable, and inexpensive.

1.2 Gas Chromatography

Gas chromatography (GC) is one of the most employed analytical separation methods in the world today. It is a widely popular technique in a variety of industries, including pharmaceutical, environmental, forensics, oil and gas, and food sciences[13–17] for the determination of volatile organic compounds, including organonitrogen species.[18] In general, GC describes a separation method which makes use of intermolecular interactions between analytes and a stationary phase to separate compounds in a mixture as they travel via an inert, gaseous mobile phase (carrier gas) through the separation column.[19] The stationary phase itself may be either a solid or a coated liquid in composition but relies on this principle regardless.

The invention of GC is primarily attributed to the work of James and Martin in 1952.[20] Since its inception, advancements in technology and research have led to steady developments in instrument components and in turn, improvements in performance.

Despite this, the role of GC and its respective components have stayed remarkably consistent: an inert carrier gas for analyte transport, a heated sample inlet for analyte introduction and vaporization, a heated column for separation, and a detector for analyte identification. A typical setup is shown below in Figure 1-1.

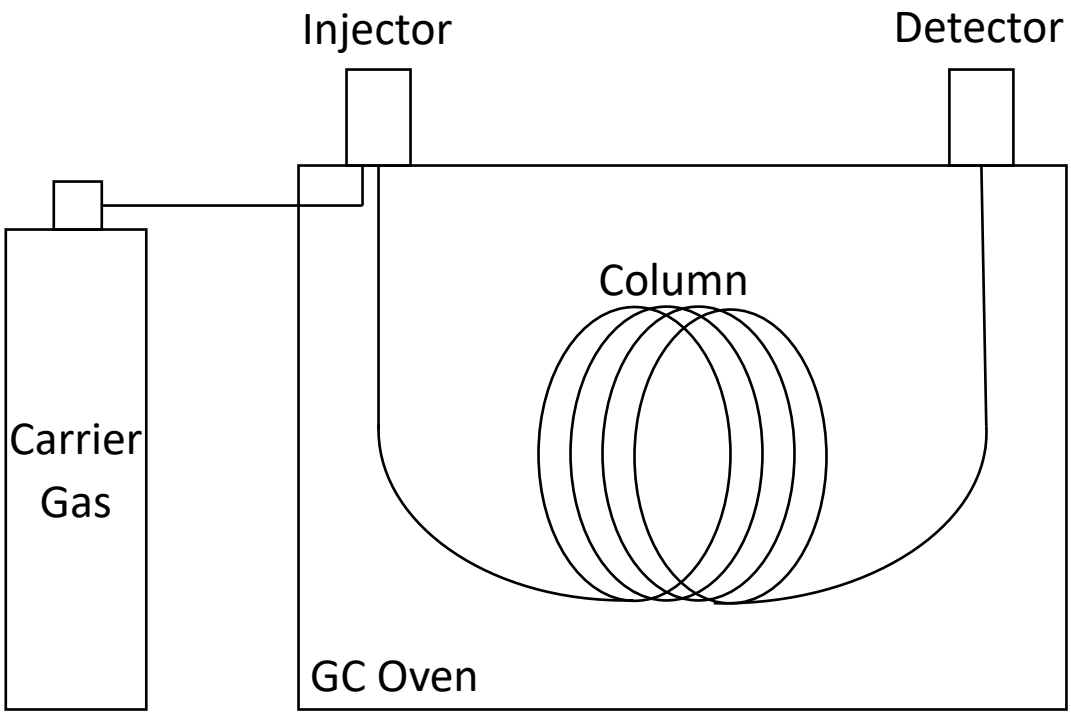

Figure 1-1: A general schematic diagram of a conventional GC system.

Over the decades, developments of the individual GC elements have allowed it to be applied to various applications. More recently, however, smaller, cost-effective and more portable detection systems have been the focus of research[21,22] as conventional GC systems are notoriously large, bulky, and, depending on certain components used, expensive. Additionally, due to the immobile nature of these systems, the process of obtaining a sample in the field, transporting the sample, performing any sample preparation

steps, and finally running the sample on the GC itself takes a significant amount of time and money. The ability of a detection system to be taken into the field to do direct sampling and testing minimizes this process dramatically. One potential area of research has been the development of sensor-based systems which primarily focus on using just the GC detector as a standalone device. Given that the detector itself can be used to obtain both quantitative and qualitative information about an analyte and that it is only a small part of the entire GC system, this remains a promising field of research. The work presented in this thesis will primarily focus on the use of GC detectors as an isolated device (i.e. without GC) to perform direct analyte analysis. As such, this will be discussed in greater detail below.

1.3 GC Detection Classifications

In every GC system, an analyte is ultimately directed to a detector, where it produces a signal proportional to the amount present. A large number of GC-compatible detectors are currently available, each based on diverse detection mechanisms for various compounds.[19] As such, GC detectors are categorized based on these principles so that one can select the appropriate detector depending on the analyte of interest as well as other physical and chemical properties of the sample.

1.3.1 Selective and Universal Detectors

In broad terms, the primary response of a detector can be categorized as either universal or selective. A universal (or non-selective) detector can theoretically respond uniformly to all (or a large subset of) analytes. In contrast, a selective detector responds preferentially to specific molecular, elemental, or chemical properties of one compound over another. For example, the flame ionization detector (FID) is deemed a universal detector, as it responds uniformly to nearly all organic compounds.[19] Conversely, the flame photometric detector (FPD) is a selective detector, being primarily sensitive to sulfur- and phosphorus-containing species.[23]

Both detector types have respective advantages depending on the nature of the analysis. Universal detectors can be useful in screening an unknown mixture to quickly gain qualitative and quantitative information about the sample, such as how many compounds are present and in what amounts. Selective detectors, on the other hand, are particularly useful in providing information about select unknown compound content as well as highlighting detector-specific analytes while minimizing background matrix signals in complex sample mixtures. The research presented in this thesis is based on the latter of these two detector types and will be expanded on later in this text.

1.3.2 Concentration and Mass-Flow Detectors

Another useful classification of GC detectors is whether a detector is mass-flow or concentration sensitive. This distinction is based on how a detector responds and quantifies an amount of analyte going through it. Concentration-sensitive detectors generate a signal proportional to the concentration of the analyte (i.e. the amount of analyte per unit volume of carrier gas) as it passes through the detector cell.[24] An example of this is a thermal conductivity detector (TCD), where the detector response is proportional to the mole ratio of the analyte to the carrier gas. A detector that is mass-flow sensitive instead responds to the total amount of analyte reaching the detector per unit time or rather to the rate of analyte introduction, regardless of the concentration.[24] This means that this type of detector relies on the elution rate of the analyte from the column and, therefore, the amount of analyte moving through the detector cell per unit time. Examples of this include both the FPD and FID.

To better understand these two designations, it can help to envision the changes to peak heights and areas as the flow rate of the carrier gas changes. For concentration-sensitive detectors, the signal height is proportional to the amount of analyte per unit volume of carrier gas. Therefore, when the flow rate of the carrier gas is increased or decreased, the concentration of the analyte remains essentially the same, and subsequently, so does the peak height. However, the peak width (elution time through the detector, and hence area) will respond to a change in carrier flow as this impacts how long the sample remains in the detector cell. Conversely, the peak height of a mass-flow sensitive detector does vary with changes in carrier flow because as the flow rate changes, so does the mass of analyte in the detector cell for a given amount of time. By contrast, the peak area will

remain the same because the same analyte mass is delivered over the time width of the peak regardless of changes in flow.

This characteristic is, therefore, important when directly comparing these two types of detectors. For example, when investigating the detection limits of a TCD, the units are reported in terms of concentration (e.g. g/mL), whereas a mass-flow sensitive detector like an FID would report detection limits in the mass of analyte per unit time (e.g. g X/s, where X is the particular element or compound responsible for generating a response).[23] As such, the flow rate and/or peak width is normally involved in comparing the performance of each.

1.3.3 Destructive and Non-Destructive Detectors

One final classification of GC detectors is destructive and non-destructive detectors. In a destructive detector, the analyte undergoes an irreversible chemical change, whereas the analyte in a non-destructive detector remains in its original form throughout the detection process.[19] The latter offers a substantial advantage if the analyte is needed for further analysis in another serial detector. However, one way of utilizing a destructive detector in this manner is to split the effluent stream coming off the column, sending one part to the detector and the other to be collected or to a separate detector in tandem for further characterization. Obviously, this only works given the analyte is present in high enough quantities, but this technique can be used to gain several pieces of information for a single injection. Destructive detectors include most flame-based detectors such as the FID and FPD, while examples of non-destructive techniques would be a TCD or possibly an electron capture detector (ECD).

1.4 Detector Characteristics

Like any other analytical technique, the characteristics of the detector are used to determine its applicability and usefulness for certain tasks. Many features of a detector, such as robustness, need for sample preparation, cost, time savings, and size, are often considered when selecting a detector. However, when characterizing a detector, there are specific, quantifiable attributes that are often reported to gauge its efficacy. Additionally, these characteristics allow detectors to be intrinsically compared to one another, regardless of the detection mechanism the detector is based on. These attributes include sensitivity, detection limits, selectivity, linearity, equimolarity, and reproducibility. To give context for the values and figures presented in this work, these characteristics will be further discussed below.

1.4.1 Sensitivity and Detection Limits

In most areas of analytical testing, detection of trace amounts of various analytes is often desired. Thus, detectors with high sensitivity and low detection limits are important attributes when choosing a detector. Sensitivity is the signal per unit concentration or mass-flow of analyte coming through the detector.[25] This definition directly refers to the ability to discriminate between small changes in analyte amounts but does not explicitly deal with the smallest amount of analyte that can still be measured. Sensitivity largely ignores the fact that analytical detectors still produce a background signal even when no analyte is present in the system. This background signal, otherwise known as noise, is the random variation in the baseline owing to sources inherent to the detector and its surroundings that

can be minimized but not eliminated. Therefore, to assess detection limits, both the signal and the noise must be considered.

Noise can be measured as either the root-mean-square noise (N_{rms}) or peak-to-peak noise (N_{p-p}). N_{rms} is calculated as the standard deviation of background deviations over a representative baseline. N_{p-p} instead is the difference in maximum and minimum deviations from a representative baseline. Generally, N_{rms} is ~5 times less than N_{p-p}.[26] The representative baseline used in these calculations is often equivalent to a time spanning at least ten analyte peak base widths. Once the noise of a system is quantified, the limit of detection (LOD) can be found using the signal-to-noise ratio (S/N), which increases with the sensitivity of a system. At trace analyte levels, the LOD is commonly found when the signal response is twice that of the N_{p-p} ($S/N_{p-p} = 2$). Alternatively, IUPAC defines the LOD as when the signal is equivalent to triple the N_{rms} ($S/N_{rms} = 3$ or $S = 3\sigma$). Detection limits are often regarded as one of the most important characteristics of a detection technique and are essential in characterizing and assessing both new and old detection methods.

1.4.2 Selectivity

As previously described, selective detectors elicit an enhanced response to certain atoms, functional groups, or chemical properties while maintaining a decreased or nominal response to the vast majority of other species. Selectivity or specificity refers to the ability of a detector to respond significantly to one compound over another. As such, formal reporting of selectivity is typically stated as the ratio of the target compound response to that of the interfering compound in orders of magnitude. For example, the FPD, which is

selective for phosphorus but indiscriminate to purely organic species, yields a selectivity of 5 x 10^5 g C/g P.[25] This means that to generate an equivalent signal to 1 g of phosphorus in the FPD, 5 x 10^5 g of carbon is needed. Or, more eloquently, 2 µg of phosphorus gives the same response as 1 g of carbon in the FPD. It is worth noting that these ratios are predominantly expressed in terms of mass of the responding element (g X) rather than in terms of the analyte compound itself. This is done simply by convention as well as to give a direct comparison of methods while accounting for disparities in weight % of the target atom to the rest of the compound.

1.4.3 Linearity, Equimolarity, and Reproducibility

An important detector characteristic is the linearity of the detector. This refers to the ability of a detector to generate a response proportional to the amount of analyte where this correlation happens to follow a straight line. Ideally, this range is perfectly linear (i.e. constant slope) at all analyte amounts, in which case sensitivity becomes independent of the amount of analyte. However, detectors have an upper limit where sensitivity falls off and plateaus due to the detector response becoming saturated from an excess of analyte. The region where the signal response is linearly correlated to analyte amount is known as the linear range. Similarly, the dynamic range of a detector is the region where a change in analyte amount causes a noticeable change in response, regardless of proportionality. An effective way to visualize these concepts is a calibration curve (Figure 1-2).

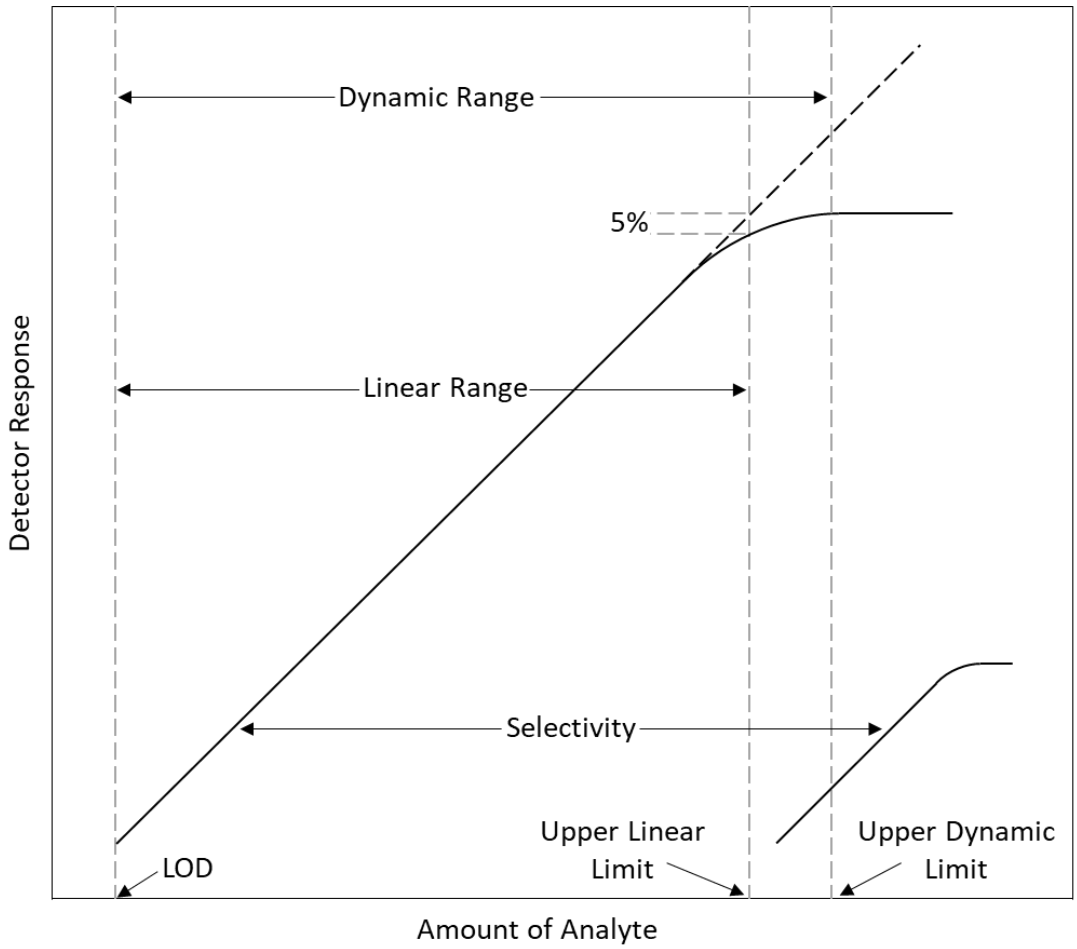

Figure 1-2: A depiction of a generic calibration curve of a detector illustrating selectivity, linear and dynamic ranges, and limit of detection (LOD).

As seen above, detector response changes as a function of analyte amount. The slope of this line (sensitivity) is constant from the LOD to the upper limit whereupon the detector becomes saturated and no longer registers a change in response to increased analyte (dynamic range). A deviation of ≥5% from linearity is considered the end of the linear range.[25] Detectors with large linear ranges are often favored because they allow for a wide range of analyte concentrations to be analyzed. It is worth noting that some detectors do not exhibit linear response (e.g. sulfur detection in FPD), but they can still be calibrated to quantify the sample.

Another important concept when investigating linearity is equimolarity. An equimolar detector is one that yields an equal response per mole of the responsive element regardless of the molecular structure of the analyte. For example, the sulfur chemiluminescence detector is known to exhibit an equimolar response to any sulfur compound since it first converts these compounds to a common intermediate chemiluminescent species.[27] Conversely, the FPD does not give an equimolar response for sulfur compounds as response has been seen to vary significantly to analytes with different structures.[28,29] This feature can be very useful as it allows for the use of a single calibration standard for a diverse group of analytes rather than needing to calibrate for every single analyte tested.

Lastly, one must consider the reproducibility of a detector. Reproducible detectors exhibit a reliable and consistent response to an amount of analyte in run-to-run and day-to-day operations. Often, reproducibility is denoted as the percent relative standard deviation (%RSD) of these measurements. However, other measurements, such as the ratio between analytes can also be helpful in %RSD calculations. For example, if signals for replicate injections of two analytes change over time, one could take the ratio of the area or height of the two analyte peaks. If the ratio stays consistent, this indicates that all signals are being inherently biased in a similar manner which may be external to the detector. The lower the %RSD, the more reproducible a response.

1.5 Flame-Based GC Detectors

As mentioned previously, currently available GC detectors are based on numerous detection mechanisms. Regardless of the mechanism employed for detection, flame-based detectors are a group that rely on the use of a flame supplied by a composition of gases (hydrogen, oxygen/air) as a means to reduce, ionize or otherwise breakdown an analyte to a specific form whereupon it can be detected or undergo further reactions to form a detectable species. This is to say that most, if not all, flame-based detectors are destructive in nature. Nevertheless, this group of GC detectors are some of the earliest developed and remain among the most widely used today. They possess attractive features such as high sensitivity, selectivity, and linearity, as well as being robust, reliable, and simple in design and use. Several are also known to provide excellent detection towards heteroatomic species. Below are some relevant examples of flame-based GC detectors.

1.5.1 Flame Ionization Detector

The flame ionization detector (FID) is one of the most widely used detectors in GC. It was simultaneously developed by both McWilliam and Dewar,[30] and Harley et al.[31] in the late 1950's and soon after became commercially available for GC. As mentioned previously, it is a universal, mass-flow sensitive detector used in the detection of organic compounds. The FID consists of a stainless steel (SS) flame jet coupled to an applied voltage (i.e. flame "polarizer") that the column effluent is fed through. A cylindrical collector electrode usually held at ground is placed downstream from the jet, inducing an electric potential across the flame. The basic design of an FID is shown in Figure 1-3.

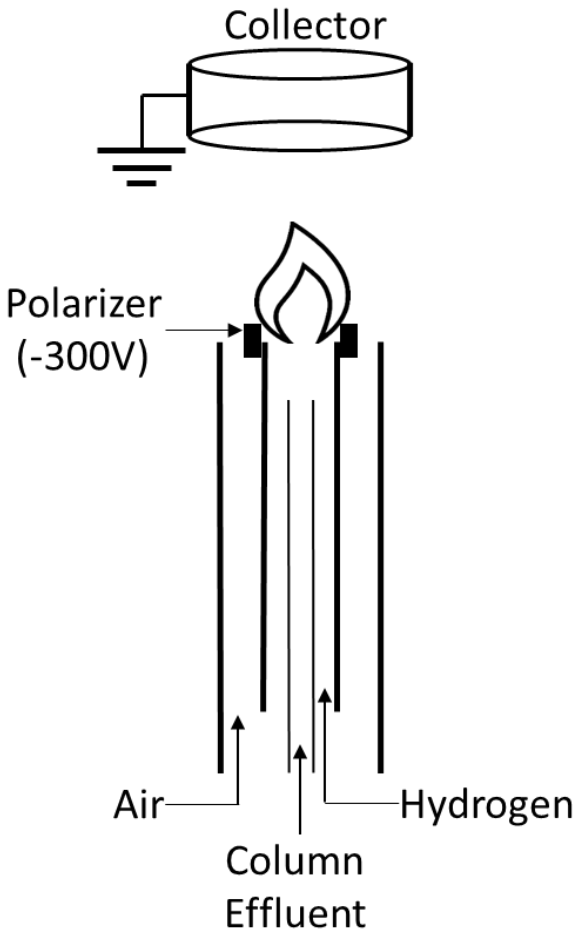

Figure 1-3: A general schematic diagram of an FID.

The operating principle of the FID relies on the use of the air/hydrogen flame to break down and ionize the eluting organic species to produce charged species which are then drawn to the collector electrode due to the potential difference where they produce a detectable current. While the mechanism itself is not entirely understood, it is generally accepted that CH· radicals are produced by the combustion of the organic species in the flame. From here, chemi-ionization reactions with oxygen radicals form a CHO^+ ion and an electron via Equation 1 as seen below.[26,32]

$$CH^{\cdot} + O^{\cdot} \rightarrow CHO^{*} \rightarrow CHO^{+} + e^{-}$$ **Equation 1**

These charged species are believed to be the responsible charge carriers related to current generation in the collector depending on the polarization of the two electrodes. Remarkably, the ionizing efficiency of the flame is relatively low, with only ~1 in 10^6 carbon atoms producing an ion.[26] Despite this, the FID has excellent sensitivity and linearity, able to detect single picogram levels of carbon per second (10^{-12} g C/s) with a linear response range of up to seven orders of magnitude.[19] Furthermore, due to the reduction of all organics to single-carbon fragments, FID response is notably equimolar and reproducible since the current generated is proportional to the number of carbon atoms coming through the detector.[32] These attributes, in addition to low maintenance requirements, cost, robustness, and simplicity, have cemented the FID as an industry standard detector.

Without additional instrument modification, the FID produces weak or nonexistent signals for inorganic species, heavily oxidized species (CO, CO_2, formic acid), or water. This is due to analytes needing a hydrocarbon component in order to generate CH· radicals, as well as the inability of these oxidized species to ionize in the flame. Organic compounds with certain heteroatoms, such as nitrogen, oxygen, sulfur, and halogens, are still detectable, though have been seen to yield a slightly lower response. This is likely because of the competition of these atoms to form other neutral species (HCN, CO) in the flame, which are not further ionized.[32]

1.5.2 Flame Photometric Detector

The flame photometric detector (FPD) is another prevalent GC detector, but for more exclusive uses. Specifically, the FPD is a selective, mass-sensitive detector primarily used in the detection of sulfur and phosphorus-containing compounds. Developed by Brody and Chaney in 1966,[33] the basis of detection has remained relatively the same, though dual-, pulsed-, and multi-flame burner designs have been developed in an effort to combat issues such as hydrocarbon quenching and structure-specific response variations.[34–36] The FPD is based on monitoring the chemiluminescent emissions of certain heteroatoms in a hydrogen-rich flame via a photomultiplier tube (PMT). To achieve this, the main detection zone of the FPD is contained within a light-tight housing to minimize both analyte emission losses as well as false positive signals due to stray outside light. The flame itself is a relatively cool (~500°C) premixed air and column effluent mixture, burning in hydrogen. Emissions produced in the flame are then directed via a quartz light guide to the PMT, where the incoming light is amplified and quantified. Optionally, an optical filter can also be placed between the emission source and the PMT to isolate certain wavelengths produced by specific elements. A schematic diagram of a single-flame FPD can be seen in Figure 1-4.

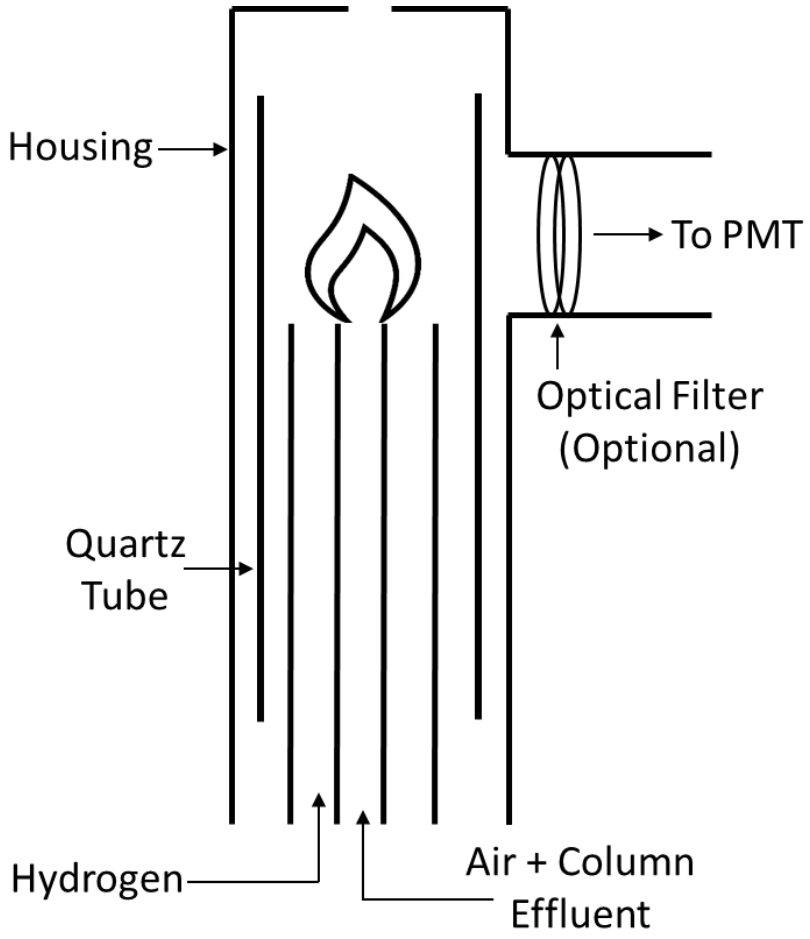

Figure 1-4: A general schematic diagram of an FPD.

Like in the FID, compounds are decomposed in the flame. In contrast to the oxygen-rich FID flame however, the hydrogen-rich plume of the FPD flame allows for an abundance of hydrogen radicals. Although specifics are not entirely understood, these hydrogen radicals, in addition to the reduced heteroatomic analyte fragments, are acknowledged to assist in the formation of the emitting species while also providing the energy necessary for its excitation and subsequent emission through radical recombination reactions.[32] For sulfur-containing compounds, they are first decomposed to compounds such as H_2S, HS, S, S_2, SO, and SO_2 depending on flame chemistry. These reduced species

then undergo several two- or three-body collision reactions to produce an excited state species, mainly S_2^*, which can relax, resulting in a broadband emission from 320 to 460 nm with a maximum emission at 394 nm.[25] This excitation mechanism is not specific to sulfur, as any chemiluminescent species can utilize these reactions with hydrogen radicals. In the case of phosphorus-containing species, the primary emitting species produced is HPO^*, with a characteristic emission maximum at 526 nm.[19,33]

Due to the complexity of flame chemistry and the potential for various chemiluminescent species to form, species-dependent light emission greatly impacts detector response. For phosphorus, where HPO^* is the main emitting species, the response is proportional to the number of phosphorus atoms entering the flame and therefore forms a linear correlation. However, the emitting species for sulfur is largely S_2^*, which requires two sulfur atoms for emission. This response is inherently non-linear and is theoretically quadratic (Equation 2), but in practice, values for n have been seen to range between 1.6 to 2.2.[25,28,29]

$$Response \propto [S]^n, where\ n \cong 2 \qquad \textbf{Equation 2}$$

Evidently, the FPD's greatest strength is its selective response for target analytes over potential interfering compounds in the bulk sample matrix. Typical single-flame FPDs have a selectivity for sulfur over carbon (S/C) of 10^4-$10^{6,}$ with pulsed-flame burners able to reach levels of $>10^7$.[32] Phosphorus response in all burner types is less variable, with a P/C of 5 x 10^5 and, due to the linear response curve, a linear range of up to five orders of

magnitude.[25,32] Irrespective of species-dependent emission disparities, the FPD also has excellent sensitivity with typical detection limits ranging from 0.5-0.01 pg P/s for phosphorus and 50-1 pg S/s for sulfur.[23,32]

As mentioned previously, the FPD is mainly used for phosphorus and sulfur detection; however, many other heteroatoms have been explored and are known to produce quantifiable emissions.[37–39] Organonitrogen species have been seen to give some measurable response, albeit with relatively weak intensity. Furthermore, the spectral range of these compounds happen to overlap with the emission profiles of several other important atoms.[39] This limits confidence in using the FPD as a nitrogen-selective detector as it struggles with identifying these species over background organic compounds.

1.5.3 Alkali Flame Ionization Detector

The alkali flame ionization detector (AFID) is a type of thermionic emission detector (TID) first invented for GC in 1964 by Giuffrida and Ives as a means for organophosphate pesticide determination.[40,41] Since then, several other heteroatoms have been found to be selectively detected, with nitrogen and phosphorus being the main species detected using the AFID.[42–44] Essentially, the AFID is a modified flame ionization detector (FID) that incorporates an alkali salt between the polarized flame and the downstream collector electrode (Figure 1-5). Numerous types of alkali salt and approaches of integrating it into the flame have been tested,[42,45–47] but all these variations primarily rely on the same general scheme of the heated salt interacting with the analyte as it is being decomposed in the flame. As a quick aside, in recent decades the term TID has been

generally associated with the nitrogen-phosphorus detector (NPD). The NPD is a more modern version of the AFID, using an electrically heated ceramic bead to introduce the alkali salt into the detector rather than a flame. As such, most modern literature describes the NPD rather than its original version, the AFID.

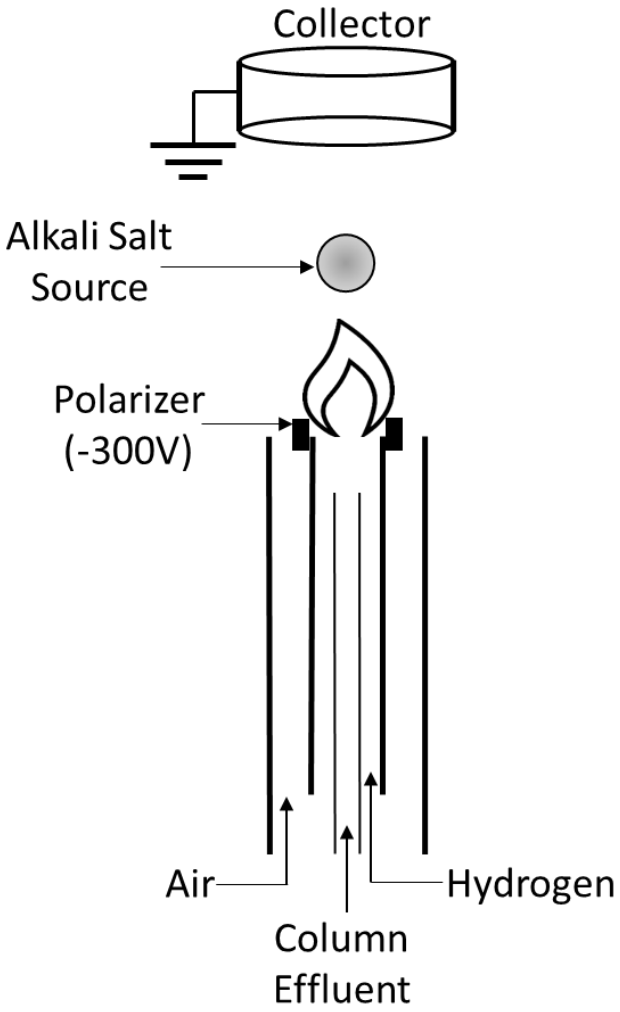

Figure 1-5: A general schematic diagram of an AFID.

Like the FID, the AFID is also an ionizing detector, relying on the current produced by ions in the flame at the collector electrode. However, the mechanism responsible for signal generation in TIDs is quite dissimilar and much less understood. Currently, it is believed that nitrogen and phosphorus compounds entering the flame decompose and form products with high electron affinities (CN·, NO_2·, PO_2·). These precursors are then thought to undergo certain reactions with the alkali metal ions to produce the negative ion products (CN^-, PO^-, PO_2^-, PO_3^-) responsible for the enhanced detector response observed from these analytes (Equation 3).[48,49] The specific mechanism whereby these precursors become fully ionized is still heavily debated, with the two prevailing theories unsure if reactions between these fragments and the alkali metal occur in the gas phase or at the surface of the salt source.[25,48,50–52]

$$CN\cdot + Rb\cdot \rightarrow CN^- + Rb^+$$ **Equation 3**

As briefly stated, the AFID has seen countless iterations in architecture, which has allowed for some degree of tunability toward certain compounds and detector characteristics. The AFID is largely noted to be selective to phosphorus and nitrogen species but has shown a preference for sulfur and halogens in some systems.[53–57] One topic of research exclusive to AFIDs is how salt composition influences detector specificity. Generally, it has been found that rubidium salts give the largest enhancement for organonitrogen compounds, while potassium salts were better for phosphorus species.[43,54] The salt anion was found to be less important to selectivity, however, variations in salt

volatility are known to impact background noise.[54] While the salt is responsible for signal enhancement, a recurring issue with all TID detectors is the expenditure of the alkali salt and eventual loss in sensitivity and selectivity. Early AFIDs expired within several days while more modern designs have been noted to last months.

Despite these issues, the AFID maintains excellent selectivity and sensitivity. As mentioned, the AFID is selective to mainly nitrogen and phosphorus, with phosphorus being 10-100 times more selective than nitrogen.[42,44,54] Selectivity is known to again vary between systems and differences in parameters, especially hydrogen flow.[54] Regardless, nitrogen has been seen to be ~100-1000 times more selective over carbon with a detection limit of around 10 pg.[43,44]

Linear response in the AFID was often debated early on, with some sources indicating an equimolar response in their system for specific analytes, while others were unable to support this notion of proportionality.[56] It is now generally supported that the AFID does exhibit a linear response, whereas early systems exhibited a linear range of ~10^3-10^6 depending on the analyte.[44,54,56] Newer NPD systems corroborate this notion showing linear ranges of up to five orders of magnitude.[25]

1.6 Other GC Detectors

As discussed, there are numerous commercially available GC detectors that can adequately sense organonitrogen species, such as the TCD, ECD, or NPD. Some other detectors not already mentioned are the nitrogen chemiluminescence detector (NCD) and mass spectrometry (MS). While many of these techniques are equal or superior to the

techniques mentioned above in nitrogen selectivity and sensitivity, several of these detectors rely on complex mechanisms and require specialized equipment that can often be fragile, expensive, or resource-heavy. For example, traditional GC-MS techniques are known to offer LODs in the low femtogram range, greater than five orders of linearity, and able to identify any compound regardless of structural and atomic makeup (i.e. pseudo universal detection).[16] As such, GC-MS has become one of the "go-to" analytical detection techniques in industry today. However, to achieve these attractive characteristics, GC techniques require an ionization system, a mass analyzer such as a quadrupole or time-of-flight, and to be held under ultra-high vacuum levels (up to 10^{-7} torr). These systems are complex, expensive, and prone to failure. Not to mention miniaturization of such a system is difficult and time-consuming, often at the expense of performance while remaining costly and intricate.[58]

1.7 Sensor-Based Detection

While analytical testing methods are generally confined to a lab, the samples themselves can be located from several hours to days away from the lab. Sampling and transport costs, potential sample contamination, and sample storage are all issues that drive up the expense, time, and reliability of conventional testing methods. Chemical sensors are systems developed for the express purpose of in-situ analysis as a means to remove these restraints associated with chemical testing. However, for these sensor-based detection methods to be of use, they must be portable, lightweight, cost-effective, robust, and have low power requirements while maintaining accuracy and precision constraints of

traditional testing methods. Furthermore, these systems would ideally be easy to use and service with limited ongoing costs. Several classifications of sensors exist for various applications, but for the purpose of this work, we will only examine sensors with the ability to detect volatile (i.e. airborne) analytes.

Chromatographic sensor systems, like their bench-top analogues, generally rely on separation and detection of analytes, though several systems remove separation for convenience and focus simply on detection. This can lead to difficulty in differentiating compounds and create false positives. Separation can usually be added back to these systems, though at the cost of device footprint and analysis time. Because GC is only amenable to species that can be transferred to the gas phase, many of the detectors commonly used in GC already possess the ability to detect airborne compounds without the need for prior analyte derivatization or additional components aside from sample introduction. Consequently, some GC detection methods and mechanisms have been adapted to sensor-based detection applications. FID, FPD, ECD, TCD, and MS have all been seen in portable GC systems.[59,60] FPD and photoionization detectors, in particular, have been used in airborne sensing for chemical warfare agents without any analyte separation.[11,60] Several of these systems, however, still suffer from issues of cost, bulkiness, weight, and remain complicated to operate.

Other sensor-based detection systems include ion mobility spectroscopy (IMS). One of the most used sensor-based detection methods, this technique offers excellent sensitivity and portability with short analysis times. However, IMS is prone to false positives due to poor selectivity and requires specific radioactive isotopes to enable its detection mechanism.[11,59,60] Spectroscopic systems like infrared- and Raman-based

techniques are also frequently used, as they are non-destructive and offer high sensitivity. Like IMS though, they suffer from issues with selectivity as well as detecting analytes in mixtures of background materials.[11,60]

As noted above, there are several sensor-based detection methods available for the detection of organonitrogen compounds. However, all possess one or more issues pertaining to cost, size, or complexity. As such, an inexpensive, portable, and robust method for detecting these compounds with high selectivity and sensitivity is needed.

1.8 Statement of Purpose

The research presented in this thesis will explore the construction of a novel portable sensor as a means to identify and quantify airborne organonitrogen compounds. As discussed above, organonitrogens are important in a variety of industries, and in-situ testing of these compounds is desirable. However, current detection systems suffer from being large and immobile or are overly complex in function and expensive. Conversely, flame-based detectors are largely robust, inexpensive, and rely on relatively simple design and detection mechanisms. Specifically, the AFID offers excellent nitrogen selectivity while exhibiting both picogram-level detection limits and reasonably high linear response. However, no reports exist for its implementation as an independent air sensor without GC separation. This may be partly due to the unknown response implications and potential difficulties imposed by a sensor design.

In recent years, the Thurbide group has been investigating the properties of micro-countercurrent and orthogonal flames operating in compact, lightweight, planar-channelled

formats.[61,62] This approach allows for sensitive and stable flame operation in both FID and FPD platforms, with a simple design and easy incorporation of supporting detector components.[36,63] Considering the advantages posed, the useful properties of the AFID, and the successful incorporation of other flame-based devices like the FPD into portable sensor applications, it would be interesting to examine if the AFID could be used as a direct sensor for airborne organo-nitrogen compounds.

Chapter Two outlines the experimental details as well as the detector design, including all components and construction choices. General operating parameters and procedures of the sensor will also be examined. Chapter Three explores how and why certain design features were chosen, as well as the optimization and characterization of the AFID sensor both quantitatively and qualitatively. How the detector responds to structural changes and different organic heteroatoms will be considered as well.

Based on literature reports regarding the use of FPD in a sensor-based system, this conventional detector was chosen as a means to compare the proposed AFID sensor against detection and response character. Furthermore, the coupling of two or more sensors has shown an increased ability to identify and better characterize analytes. Chapter Four examines these two concepts, as well as demonstrates how to utilize detector-specific ratios to indicate the molecular composition of a sample. The dependence of this ratio on both analyte concentration and structure will also be investigated.

Chapter Four also probes real-world applications of the proposed sensor. Specifically, how certain sample matrices impact detector response as well as the use of the device in testing of chemical warfare surrogates at equivalent levels immediately dangerous to life and health. Lastly, a summary of the presented research is described in

Chapter Five, along with thoughts regarding future work and potential additions and applications for the AFID sensor.

Chapter Two: Experimental

2.1 Instrumentation

2.1.1 AFID Sensor

Figure 2-1 displays a schematic diagram of the current AFID device, which is primarily comprised of a planar channelled face piece and a matching cover plate to seal the flow paths.

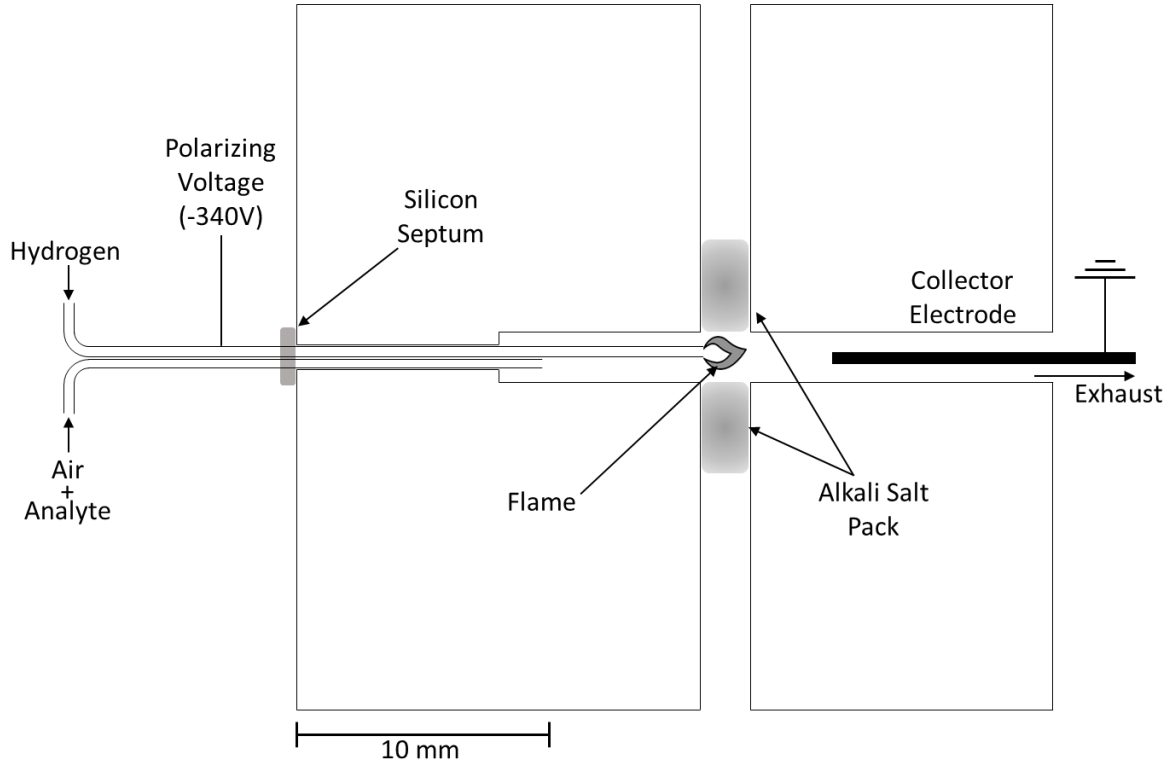

Figure 2-1: Schematic diagram of the current AFID sensor design. The primary channel (horizontal) includes introduction of flame gases and analytes, collector electrode, and exhaust. Secondary salt channel (vertical) contains packed alkali salt

The face piece (Figure 2-2) was fashioned out of a rectangular quartz block (30 mm x 28 mm x 7 mm) with precision-milled U-shaped channels cut into the surface of the block. A quartz slide (1 mm thick) cut into similar dimensions was used as the cover plate and was sealed to the face piece around the edges using a temperature-resistant UV-cured adhesive (Loctite AA 363; Henkel, Connecticut, USA). Both the face piece and cover plate were cut and shaped in the University of Calgary's glass shop.

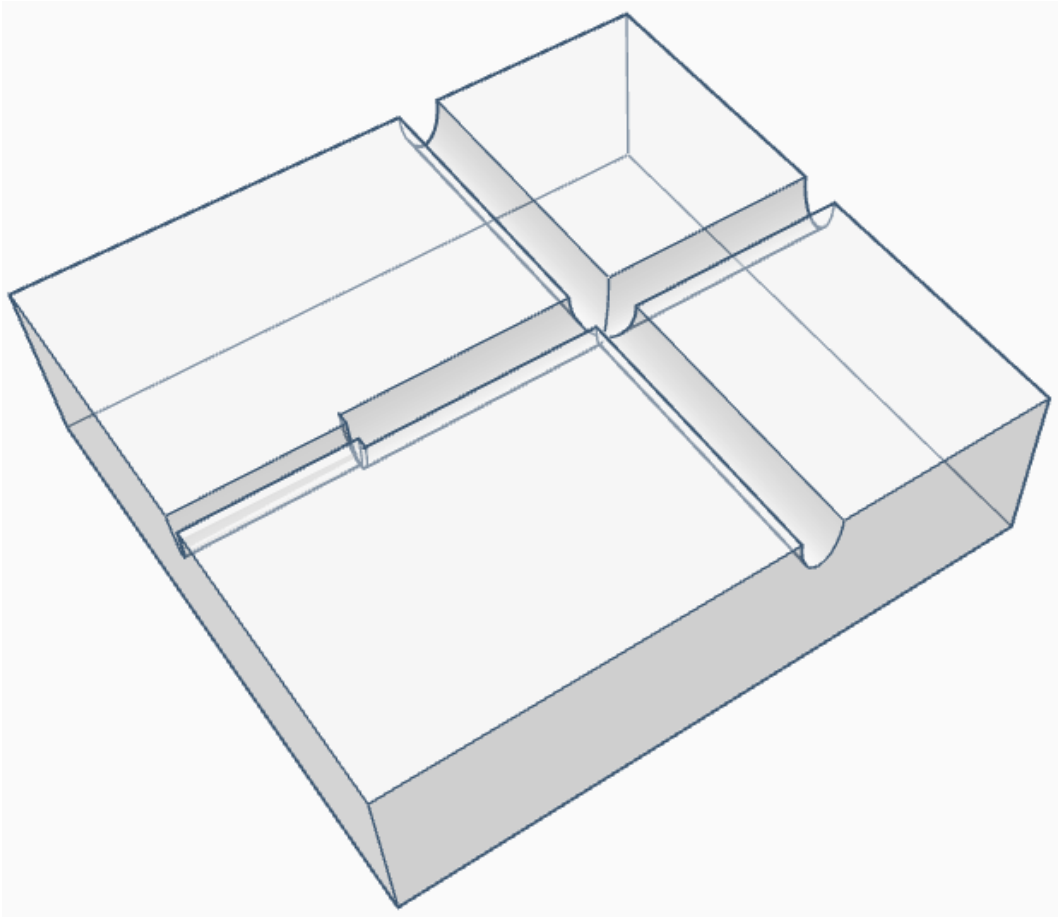

Figure 2-2: 3-dimensional rendering of quartz face piece.

On the surface of the quartz face piece (left to right in Figure 2-1), a primary channel (1 mm wide x 2 mm deep) extends 8 mm from the center of the left edge and then expands into a 2 mm wide channel (2 mm deep) for the remaining 22 mm to the right edge of the block. A second channel (28 mm x 2 mm x 2 mm) intersects the first at $90^{o,}$ about 17 mm from the left edge. This junction is where the flame resides while the AFID is operational. Two stainless steel (SS) capillaries (0.635 mm I.D., 0.813 mm O.D., McMaster-Carr, Aurora, USA) were used to introduce hydrogen and air through a high-temperature septum affixed to the left edge of the device, which was made from silicon adhesive (Permatex, Solon, USA). This provided a reusable seal around the capillaries to prevent the loss of flame gases and analyte, and guided them into the narrow end of the primary channel to support the flame and deliver analyte to the device. The hydrogen capillary terminated at the channel junction, while the air capillary normally terminated just past the expansion point of the channel. High-purity hydrogen gas (Air Liquide, Calgary, Canada) was independently delivered to the flame, while a piezoelectric diaphragm micro-air pump (model mp6-gas; Bartels Mikrotechnik GmbH, Dortmund, Germany) was used to draw ambient air and analyte into the device. Connections were made using sized Teflon tubing (McMaster-Carr). On either side of the channel junction, the supporting alkali salt was packed into the channel. An aqueous saturated salt solution was also applied and left to dry in the channel junction as a means of further introducing salt to the flame. A grounded SS rod (0.64 mm diameter, McMaster-Carr) was inserted in the right edge of the primary channel and situated ~5 mm from the flame, where it acted as the ion collector electrode while 340 V was applied to the SS hydrogen capillary to polarize the flame. The applied voltage and signal detection was performed using a standard FID

electrometer. An image displaying the AFID sensor operating under normal conditions can be seen in Figure 2-3 below.

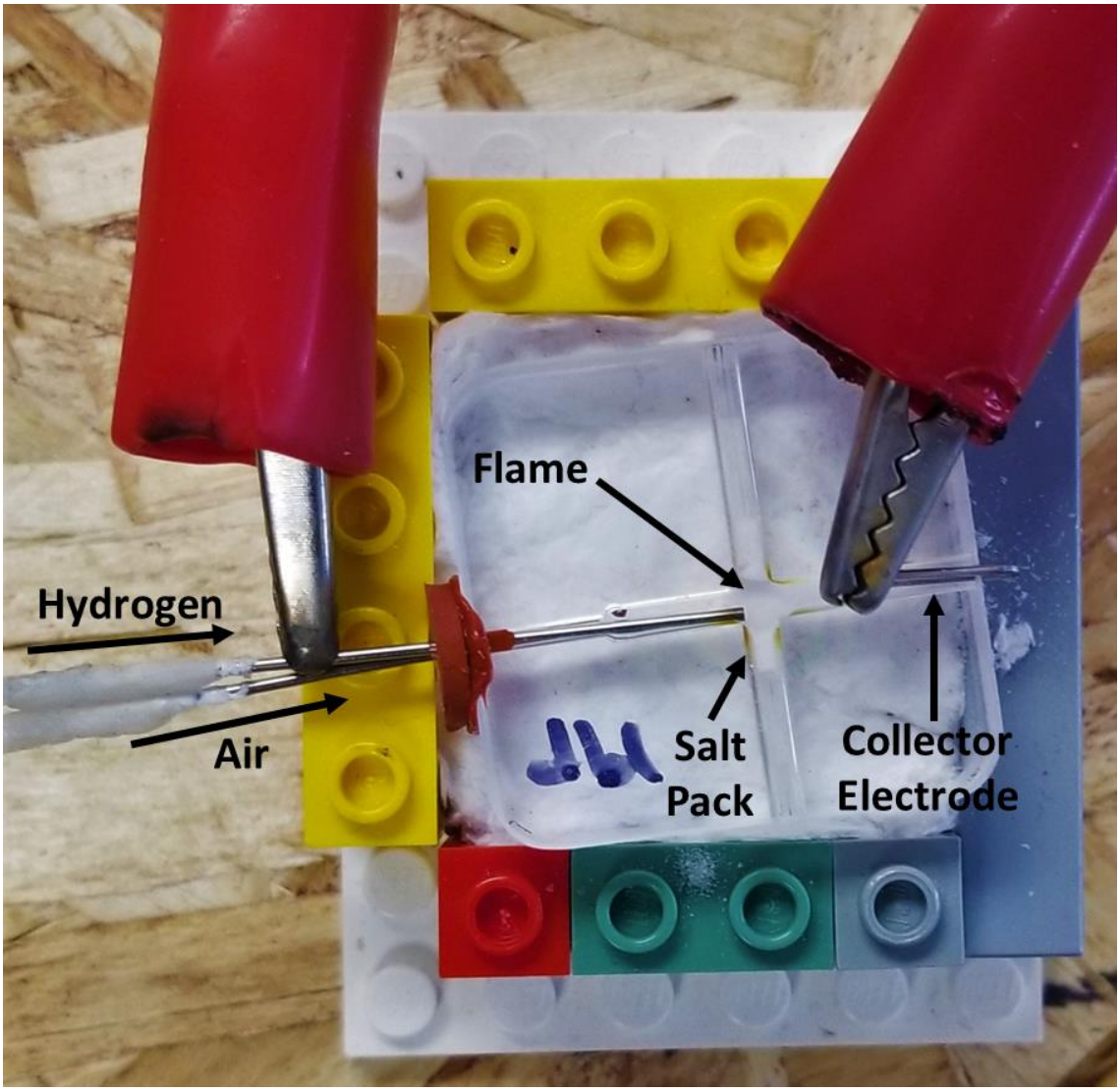

Figure 2-3: An image of the AFID sensor operating under normal conditions.

2.1.2 Tandem Detector System

For direct comparisons, a conventional FPD and the AFID sensor were connected in parallel, where a single sample inlet was split by a Teflon tee union into separate analyte flow paths leading to the respective micro-air pumps supporting each device. This simultaneously delivered analyte to each detector from the sampling bag without affecting the flow rates. The FPD was set up as a standalone detector similar to the AFID sensor (i.e. no prior chromatographic separation), where the flame was supported using high-purity hydrogen in addition to air supplied by the micro-air pump. The FPD used a band-pass filter (Model FGUV5; 240-395 nm; Thorlabs, Newton, USA) in the photomultiplier tube (Hamamatsu Photonics, Hamamatsu City, Japan) to isolate nitrogen emission bands.[39] The AFID sensor was set up as described previously.

2.2 General Operating Parameters and Procedures

To maximize its contact with the flame, the alkali salt was normally packed into either side of the channel junction before use. This was conveniently pressure-packed by hand by blocking the primary channel with a SS rod, pouring the salt powder into either side, and using a SS plunger to compress it into place. Additionally, 1-2 drops of a saturated aqueous salt solution was deposited in the channel junction by syringe then left to dry on the junction walls overnight. The supporting components were then attached to the quartz chip, and the device was preheated to 60°C using an external heating block before ignition to reduce water condensation from the flame and the background noise that it created. With hydrogen flowing through the SS capillary, a flame was established on its end by presenting

a spark at the exhaust outlet while ambient air was also drawn into the device by the micro-air pump. Optimal gas flows used were 40 mL/min of air and 14.5 mL/min of hydrogen. Within a few minutes of ignition, sample bags were typically connected to the inlet of the micro-air pump for a duration of 30 seconds to achieve a signal plateau in the sensor. To clean the AFID sensor, deionized water and a Teflon brush were used to remove any trace of residual salt before repacking.

For the tandem detector system, the AFID was operated as portrayed above. The FPD was also preheated to 80℃ to limit condensation upon ignition. To generate the flame in the FPD, a spark was presented at the exhaust outlet while flame gases were established. Optimal flow rates used were 27 mL/min of air and 16 mL/min of hydrogen, as determined by prior testing. Within a few minutes of ignition, sample bags could be connected to the sample inlet tee for a duration of 30 seconds unless otherwise stated to reach a signal plateau.

The sample bags used for testing were 1 or 10 L Teflon bags equipped with a 2-in-1 polypropylene on/off valve with a spout and replaceable, gas-tight septum (Figure 2-4).

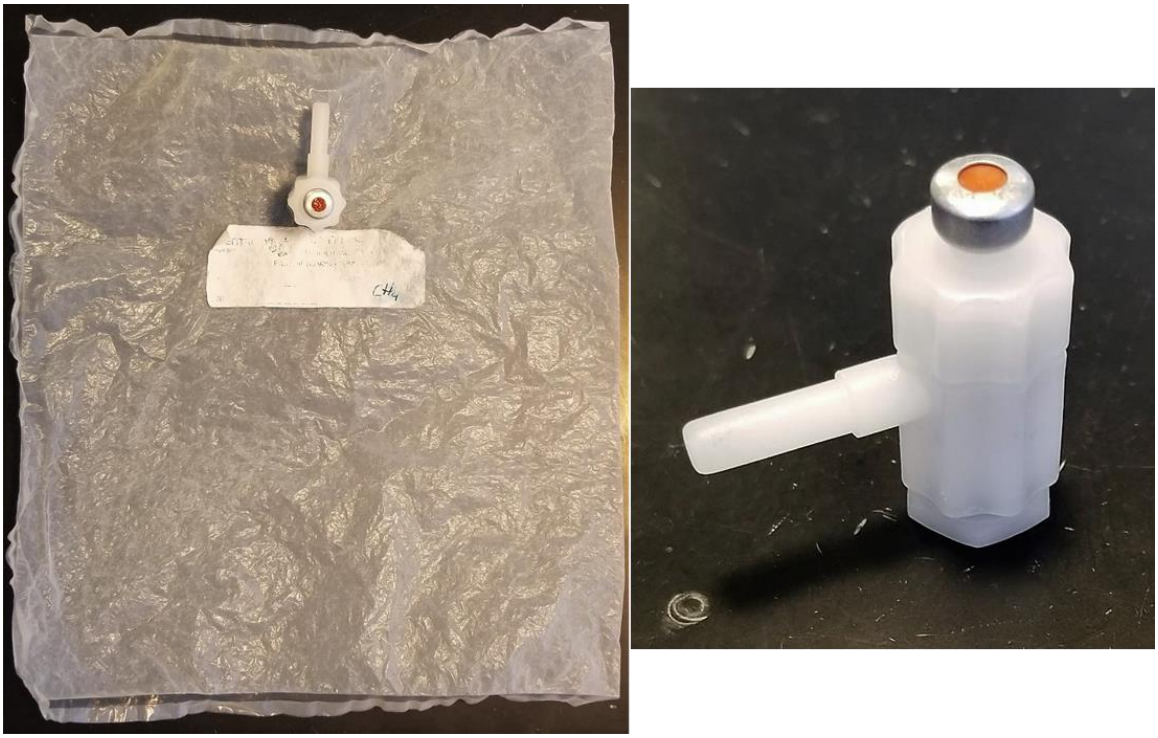

Figure 2-4: Images of sampling bag used for testing (left) and on/off valve (right).

To prepare sample bags for testing, the Teflon bags were first cleaned by flushing the bag at least three times with medical-grade air to remove any trace of previous analytes and then evacuated using a vacuum. To fill either a 1 L or 10 L bag, the spout was connected to a medical air cylinder through a piece of rubber tubing and filled to 90% of the volume (900 mL or 9 L respectively). To determine the amount of air needed to achieve the fill volume, the air was set to a constant flow and timed to fill. While filling with air, known quantities of pure analyte was added to the bag using an appropriate syringe through the gas-tight septum to reach the desired analyte or elemental concentration in the bag. For example, injecting 1 µL of analyte into a 900 mL bag of air, one can use the density of the

analyte to determine the bag concentration in grams of compound per millilitre. From here, the moles of compound per millilitre and subsequently grams of element per millilitre can be calculated using the molecular weight of the compound and the atomic weight of the heteroatom. To achieve trace level analyte quantities, serial dilution of a stock bag was performed. For experiments requiring a solid sample matrix to be added to the bag prior to analyte introduction, a 7 L resealable Ziploc freezer bag was fitted with a spare on/off valve and treated in a similar manner to the Teflon sample bags. Once filled, the sample bags were left for several minutes to ensure liquid analytes had completely transferred to the gas-phase and reached equilibrium. Subsequently, the bags were attached to the sample inlet and tested. Sample bags were prepared immediately prior to any experiments to limit potential sample degradation or loss from the bags. Bags were also constantly checked for points of failure, including bag holes or leaks and deterioration of on/off valve parts.

2.3 Chemicals and Reagents

Rubidium sulfate salt (99.8%; Thermo Fisher Scientific, Ottawa, Canada) was typically used in the AFID flame. Analytes examined include high-purity methane (Praxair, Calgary, Canada), high-purity nitrogen (Air Liquide), diethylamine, tetrahydrofuran (≥99% each; Fisher Scientific, Fairtown, USA), chloroform, pyridine, benzene (≥99% each; EMD Chemicals/EM Science, Gibbstown, USA), triethylamine (≥99%; BDH Inc., Toronto, Canada), ammonium hydroxide (28-30%; BDH Inc.), methanol, acetone, hexane, carbon disulfide, trimethyl phosphite, dichloromethane, acetonitrile, propylamine, isopropylamine, pyrrolidine, piperidine, nitromethane, tert-butyl nitrite (≥97% each; Sigma-Aldrich, Oakville, Canada), and ethylamine (70% in water; Sigma-Aldrich). Stock

analyte bags were prepared by injecting known quantities of pure liquid analyte through the gas-tight septum fitting of a 1 L or 10 L Teflon sampling bag (Scentroid, Toronto, Canada) and then, as analyte evaporated, diluting it to volume using medical grade air (Air Liquide) as the balance gas to reach desired concentrations. Gasoline was purchased from a local vendor. Car exhaust was sampled from a vehicle after 15 minutes of operation. Fish meat was obtained locally, and a 10 g piece was dried overnight before use.

Chapter Three: Characterization and Optimization of the AFID Sensor

3.1 Introduction

As discussed previously, several metrics are utilized when determining the efficacy of a chemical detection system. Many of these properties can be quantitatively defined (selectivity, sensitivity, linearity, etc.) though there are several qualitative features that also need to be examined to understand how a detector responds to these variations and what are the optimal conditions for detection. Furthermore, although the proposed detection system is based on previous GC detector research, adapting this to a sensor-based system requires several alterations to arrive at design features that are best suited for such. Both qualitative and quantitative characteristics and how they shaped the development of the proposed AFID sensor are described below.

3.2 Design Considerations and Iterations

Throughout all versions of the AFID sensor, quartz was used for the main body since it is chemically inert, can operate at high temperatures, and is a good electrical insulator for related signal collection components. As well, due to the chip thickness used, it was relatively robust in daily use and not prone to breakage by thermal cycling or minor mishandling. Early on, many detector shapes and formats were briefly examined, including

open-air and tubular formats, though these versions were mainly employed as proof-of-concept models before quickly transitioning to planar-channelled formats.

Several iterations of the on-chip AFID sensor were explored regarding gas/sample input, alkali salt source, and collector electrode/exhaust layout. It was understood from initial testing that initial designs required four main components: polarized hydrogen flame, air/analyte, alkali salt, and a collector electrode. Thus, the original planar design consisted of a four-quadrant system that included air/analyte and hydrogen inlets, a salt channel opposite the flame, and an exhaust port where the collector electrode was placed (Figure 3-1).

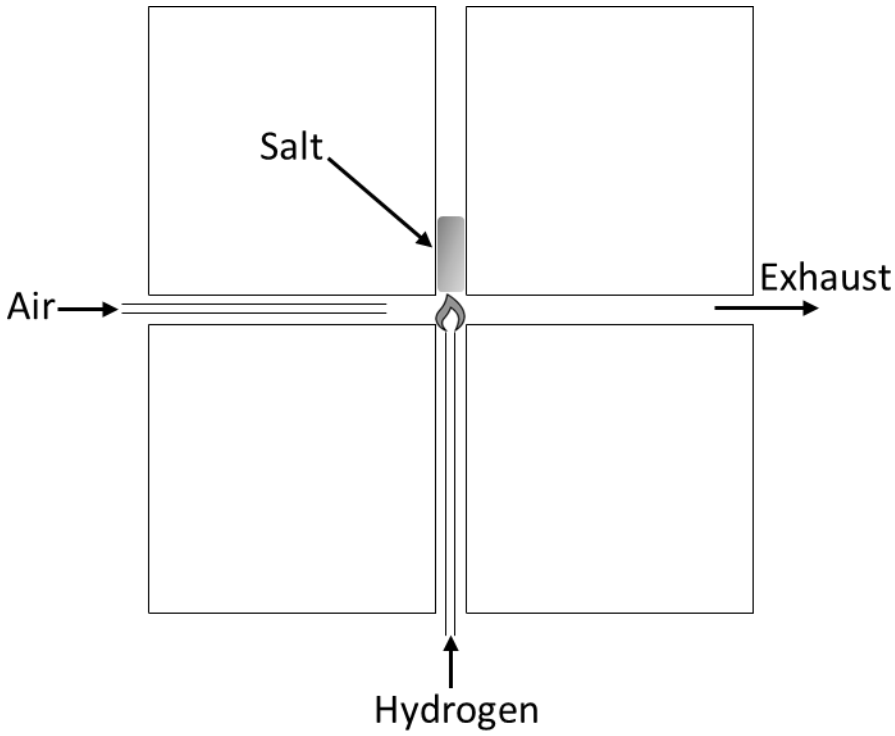

Figure 3-1: Initial design of the planar-channelled AFID.

It was noticed early on that greater interaction between the salt and the flame was beneficial to sensor performance. Therefore, the air/analyte and hydrogen inlets were consolidated into a single channel allowing for matching salt-packed channels to be arranged on either side of the centrally situated flame. This maximized salt-flame contact and linearized the path of the analyte and flame gases, resulting in a more uniform and stable flame. Several other design changes to increase flame-salt interactions were tried, including adding a third salt-packed channel, having the flame-bearing capillary cored through the salt pack, and packing SS/glass tubes with salt and placing them laterally into the flame. However, it was found that applying 1-2 drops of saturated salt solution to the channel junction and letting it dry overnight left a thin residue on the walls around the flame that best further enhanced analyte signals.

The device employed 2 mm x 2 mm channels as they were convenient to construct and maneuver during operation and allowed for consistent, stable flame operation. Decreasing the channel dimensions around or upstream of the flame would cause it to become unstable, leading to increased noise and self-extinguishing. The reduction to a 1 mm channel width at the gas inlet was found to be helpful in aligning the hydrogen and air capillaries centrally in the main channel, which supported consistent flame position within the junction. This also facilitated smooth gas flow through the main channel, minimizing flame flicker and noise. The quartz cover plate was initially annealed to the face piece, but this often led to inconsistent bonding and minor channel deformations due to the high temperatures used during the process. A UV-cured adhesive was instead used and gave a more consistent seal between the pieces without any detector interference. As such, these

aspects were incorporated into the AFID sensor design resulting in the current sensor design (Figure 2-1).

3.3 Operating Characteristics and Optimization

3.3.1 Alkali Salt Type and Procedures

As discussed, the alkali salt is the cause for analyte selectivity and signal enhancement in the AFID. Figure 3-2 demonstrates this selective response. Without salt present, similar amounts of both methane and diethylamine (DEA) yield very similar responses in this basic FID mode. By contrast, with a rubidium salt in place under the same conditions (AFID mode), the DEA signal increases to near 25 times while the methane response remains about the same.

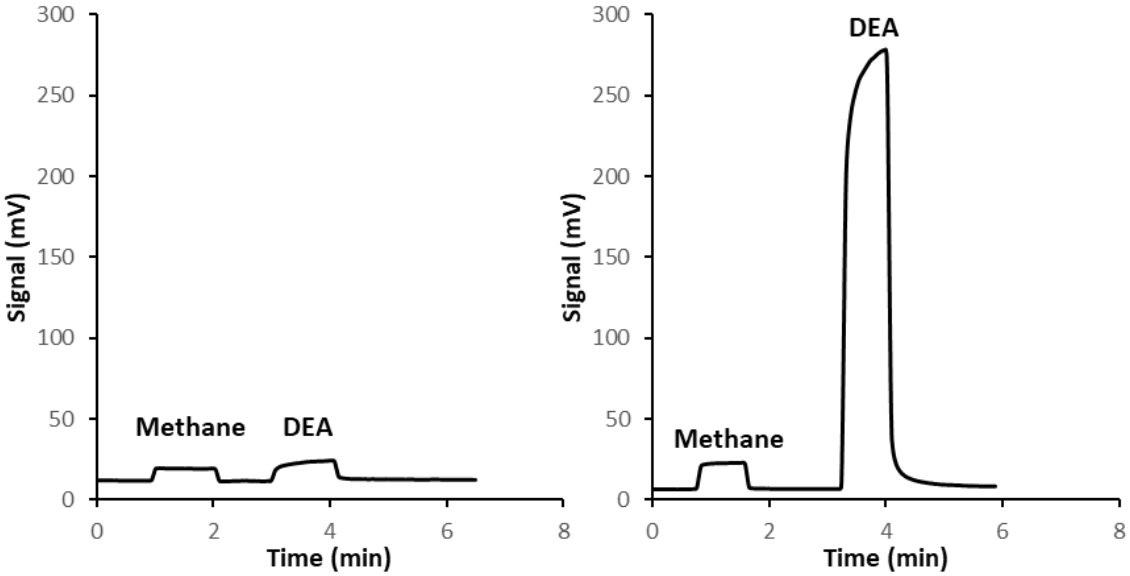

Figure 3-2: Sensor signal towards methane and diethylamine (DEA) sample bags without (FID mode, left) and with (AFID mode, right) RbCl salt present in channel.

Specifically for organonitrogen compounds, it is known that rubidium salts give the largest signal enhancement in the AFID.[43,54] As such, RbCl, $RbNO_3$, and Rb_2SO_4 were each investigated. $RbNO_3$ produced a purple flame color and a somewhat enhanced response for nitrogen analytes over hydrocarbons. However, it yielded an erratic background response, an extremely unstable baseline, and inconsistent signals. Further, it quickly disappeared due to its low boiling point of 578 °C, and so it was not used further. While RbCl showed no flame color, it demonstrated excellent nitrogen signals relative to carbon. Still, substantial erosion of the RbCl salt packs appeared over short periods, along with a brown residue in the flame channel that increased background interference and flame instability. As such, it was not pursued further. By comparison, Rb_2SO_4 also presented no flame color, but offered excellent nitrogen response relative to carbon and the most consistent analyte signals. Further, due to its low volatility (b.p. 1700 °C), no salt pack erosion or residue in the flame channel was observed. These findings agree with others who found Rb_2SO_4 to be optimal for nitrogen AFID response.[43] Note that KCl was also briefly examined and found to produce decent nitrogen response; however, it was also abandoned as it gave less nitrogen selectivity than rubidium salts, consistent with previous reports.[54]

For all salts, operating a freshly packed sensor often needed some initial conditioning prior to use. For instance, in the first few trials this usually created a large, tailing initial background response that stabilized 10-15 minutes after ignition. After this, most chips could be readily used shortly after ignition, only exhibiting a small ignition peak that quickly came back down to baseline. Additionally, it was noted condensation from the flame ignition would often interact with the salt resulting in a large, noisy signal that would

tail severely. Preheating the sensor to 60 °C was found to eliminate this occurrence and improve the overall consistency of ignition procedures.

As noted previously, salt sources are known to be consumed during AFID operation, and an eventual loss of analyte response and selectivity is normally observed with extensive usage.[64] Similarly, after continuous weekly operation of the AFID sensor here, selectivity decreases. However, it usually takes several months before significant analyte response degradation is observed. Additionally, due to the size, cost, and design simplicity, several devices can be assembled and prepared in advance so an expended chip can be easily replaced. Moreover, cleaning and repacking a used chip can be done within a day.

3.3.2 Flame Orientation and Positioning

Early testing of flame positioning and orientation was critical in determining if a sensor-based AFID was even possible. For example, rather than analyte being introduced to the flame by an inert carrier gas in GC, typical sensor architectures require analyte to be drawn into the flame along with the ambient air that also supports its combustion, which can impact molecular decomposition and detector response.[65] As well, analyte introduction is relatively transient in GC detection but more continuous in sensor modes, which can also potentially alter flame chemistry, analyte decomposition, and response. As such, several flame orientations and their relation to air and analyte introduction were examined.

Countercurrent flames, where flame gas capillaries opposed each other, were attempted in initial single-channelled versions of the sensor as these types of flames had

seen success in other detector types.[62,66] However, this style of sensor was quickly abandoned mainly due to the difficulty of salt packing in this version and the subsequent construction of the planar channelled format. Both orthogonal and linearly aligned flame-gas capillaries were attempted in the chip format as mentioned above, and it was established that having both capillaries in a single inlet minimized flame instability. Ultimately, all flame orientations were able to adequately produce analyte species and demonstrate an enhanced nitrogen response. Research into flow dynamics of the flame gases, mixing ratios, and the mechanism behind AFID response may help to better understand these impacts but were not further explored in this work.

As discussed, interactions between the flame and the alkali salt were most important in generating the enhanced nitrogen signals in the sensor, regardless of flame orientation. This concept was further illustrated when the flame was moved laterally in the main channel of the detector in relation to the salt pack. When it was situated at the downstream edge of the salt pack and then moved to the middle of the channel junction, the nitrogen response increased over 5 times Figure 3-3. This demonstrates that the body of the flame must be central to slightly upstream to the salt pack to influence and enhance signal response. Thus, flame operation in the middle of the salt pack was employed in addition to coating the flame junction with saturated salt solution.

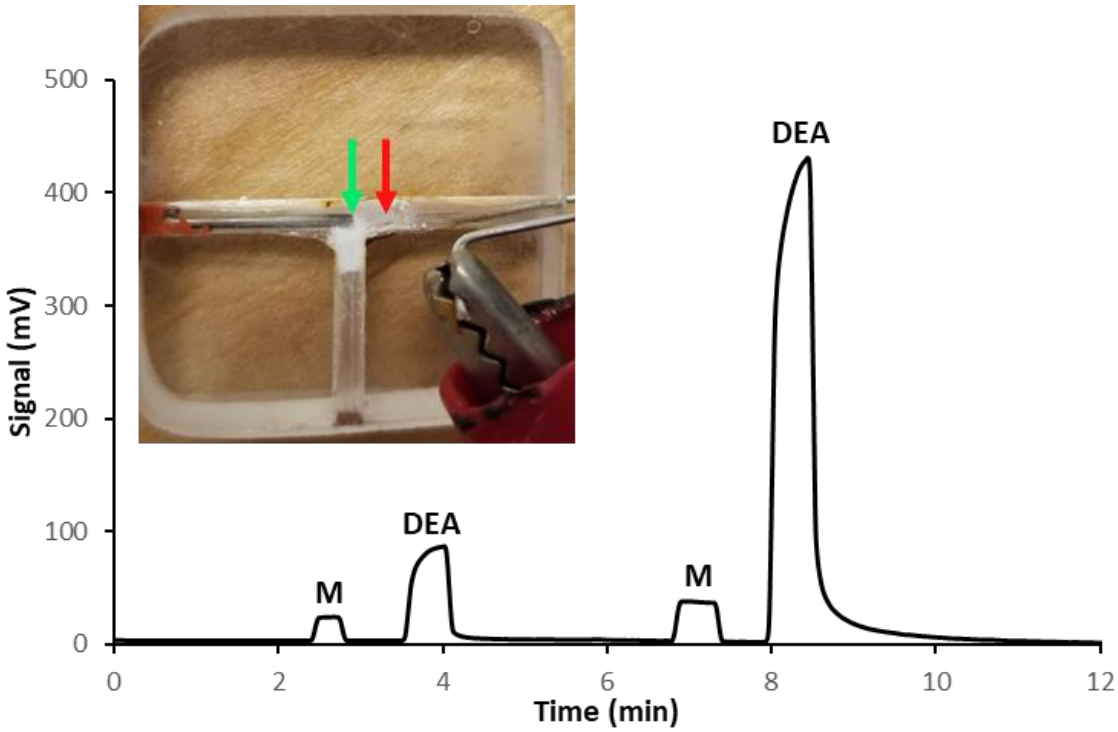

Figure 3-3*: Methane (M) and diethylamine (DEA) response in the AFID sensor as flame position is altered. Left most peaks were produced when. flame was in the position indicated in the image by the red arrow. Left most peaks were produced when flame was positioned at green arrow.*

3.3.3 Gas Flows

Gas input was next examined, where hydrogen flow showed a significant impact on sensor response. From Figure 3-4, over the range of 11 to 19 mL/min hydrogen, nitrogen response (as diethylamine) doubled and maximized between 13 and 15 mL/min. Meanwhile, methane response was relatively unchanged. Therefore 14.5 mL/min of hydrogen was used going forward to achieve optimal N/C selectivity.

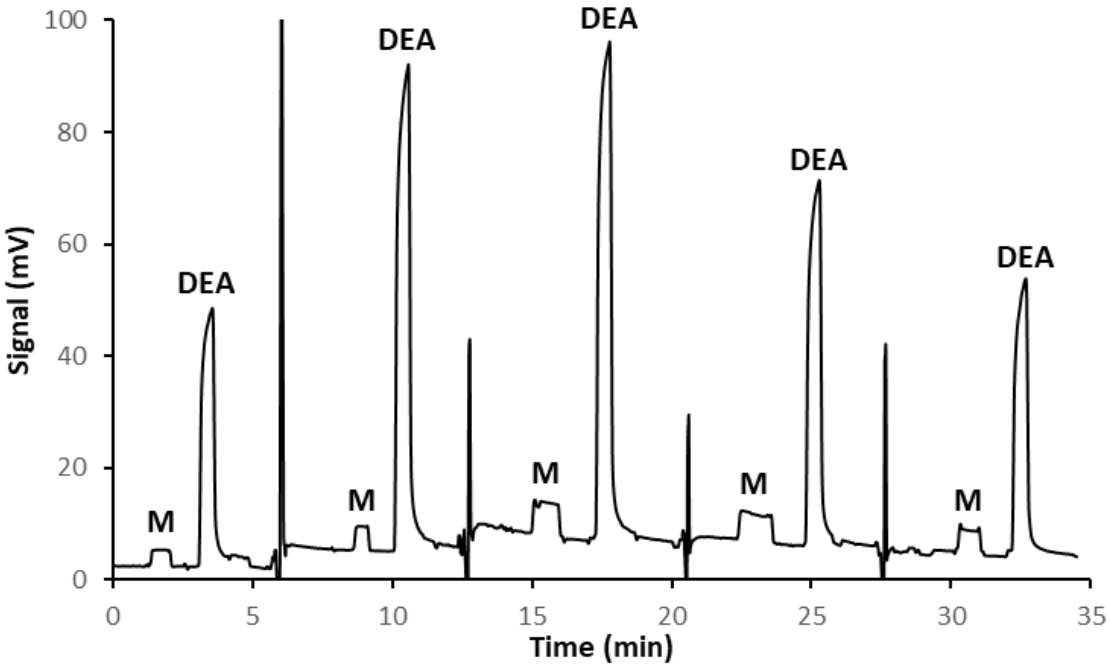

Figure 3-4: AFID response to methane (M) and diethylamine (DEA) as a function of hydrogen flow. Flows from left to right: 11, 13, 15, 17, and 19 mL/min. Intermittent spikes indicate a change in flow.

Since the micro-air pump was fixed at 40 mL/min, an auxiliary air flow from a tank source was added in using a tee between the micro-air pump and the air inlet of the sensor. In this way, when total air was increased from 40 to 80 mL/min, nitrogen response increased by only 11%, while methane was again unchanged (Figure 3-5). Given the minor benefit posed and the obstacle of adding more air to this portable device, 40 mL/min from the micro-air pump was deemed optimal for overall operation. Future devices may employ a higher flow from the air pump; however, in its current form, 40 mL/min is the upper limit of these air pumps. These findings also agree with previous AFID gas optimization reports indicating that hydrogen has a more significant influence on signals and baseline perturbations compared to air flows.[43,44] Therefore, hydrogen flow must be carefully optimized to maximize response.

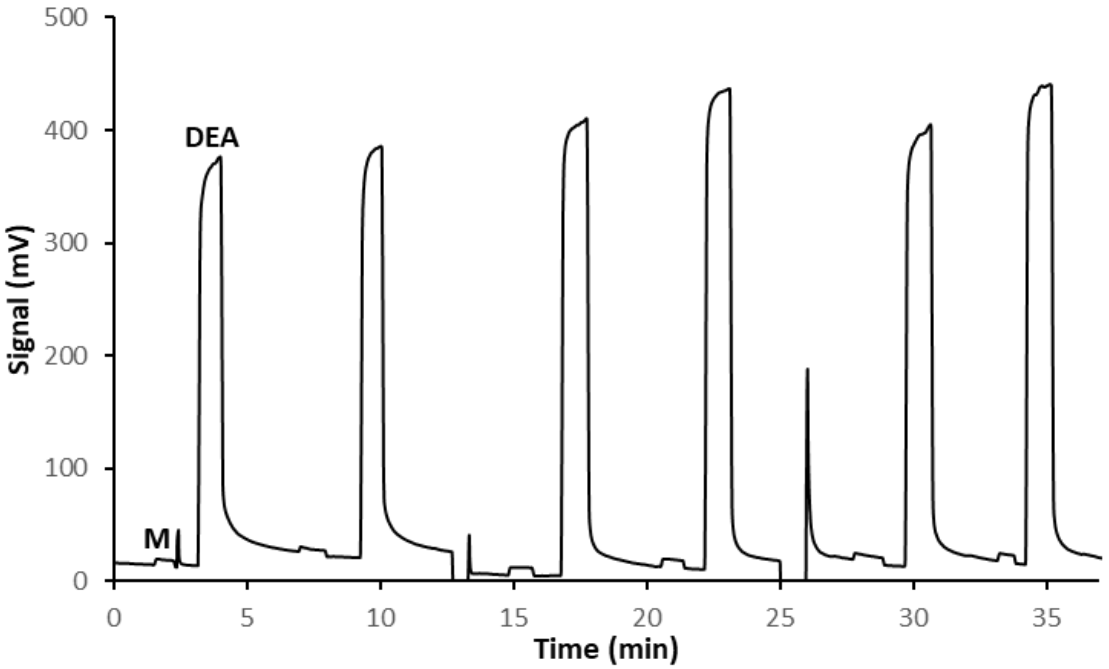

Figure 3-5: AFID response to methane (M) and diethylamine (DEA) as a function of air flow. From left to right (as doublets): 40 mL/min (pump), 60 mL/min (40 mL/min pump + 20 mL/min auxiliary), and 80 mL/min (40 mL/min pump + 40 mL/min auxiliary). Intermittent spikes indicate a change in flow.

3.3.4 Other Tests and General Traits

In addition to the parameters mentioned above, several other minor experiments were performed over the course of this research with the AFID sensor. These tests were largely qualitative in nature to gain a better understanding of the general traits and functions of the detector, as well as to ensure that day-to-day procedures were acceptable.

To confirm that daily sampling bag cleaning was adequate in removing all traces of previous analytes, bags were flushed three times and filled with medical-grade air. A blank air bag was also prepared using medical-grade air in a bag that had not been used for analyte preparation in the past. Both bags were then tested in the AFID, and their signals

compared. For all intents and purposes, flushing the bag at least three times was more than sufficient to remove all traces of analyte.

Early on, it was noticed that the AFID was sensitive to electronic sources of noise. For example, extension cords, device charging cables, and the heater block used for preignition heating of the chip could all introduce up to a ~10 times increase in baseline noise, reducing S/N values. This is expected at this stage of development, as the electrodes are essentially in open air compared to typical ionizing detectors, which are generally more insulated to limit such noise and protect the device. As such, these sources of electrical noise were moved or eliminated from close proximity to the sensor. The heater block itself was simply turned off (i.e. no applied current) after preheating the chip.

Another interesting trait of the AFID sensor is the general signal trend over time. Typically, the device exhibits slightly higher response upon ignition, and as the device remains active, signals start to depreciate and eventually taper off and plateau. Earlier versions of the sensor exhibited this behaviour to a much more extreme degree, whereas current versions only vary ~10% over the course of an hour. While this can directly affect the sensitivity of the device, unless analyte concentrations are nearing the LOD, this is typically not an issue. Moreover, this cascade seems to affect both nitrogen and carbon signals, meaning selectivity of the device stays functionally the same. The cause of this characteristic is unknown, as it has not impacted the function of the sensor significantly enough to warrant further study. It is speculated that it might be related to the thermal changes in the salt or the device itself as it heats since this has been seen to impact response.[54] It could also be due to infrequent, minor changes in hydrogen flows from day to day before readjustment. Day-to-day signal reliability was also somewhat unstable in

early models, where signal heights could vary upwards of 30%. This is not seen in current iterations of the sensor, where signals are consistent on a day-to-day basis. This reliability is likely a result of standardizing ignition procedures and limiting condensation, which was known to heavily affect the salt and ensuing signals.

3.4 Analytical Figures of Merit

3.4.1 Sensitivity and Selectivity

Using the optimized conditions above, the analytical performance of the AFID sensor was characterized in detecting organonitrogen species. As examined in Chapter One, sensitivity and detection limits are important in trace analysis and are standard benchmark features when comparing a novel detection method to a conventional one. Several calibrations were tested over various analyte concentration ranges across several days. Figure 3-6 displays a representative 6-point calibration plot of sensor response as a function of analyte concentration. DEA and methane were used as the organonitrogen and hydrocarbon compounds respectively, as these had been used in the optimization tests. As seen, the AFID sensor yields a sharp increase in nitrogen response (as diethylamine) for increasing concentrations, reflecting its high sensitivity for such analytes. As a result, the LOD of the AFID sensor towards organonitrogens was ~30 pg N/s, which correlates to sub ng/mL amounts (parts per billion level) of DEA (at 40 mL/min air/sample flow). Conversely, for hydrocarbons, the detection limit was ~2800 pg C/s. These values were determined when S/N = 2, where noise was measured peak-to-peak from a representative baseline of the AFID sensor.

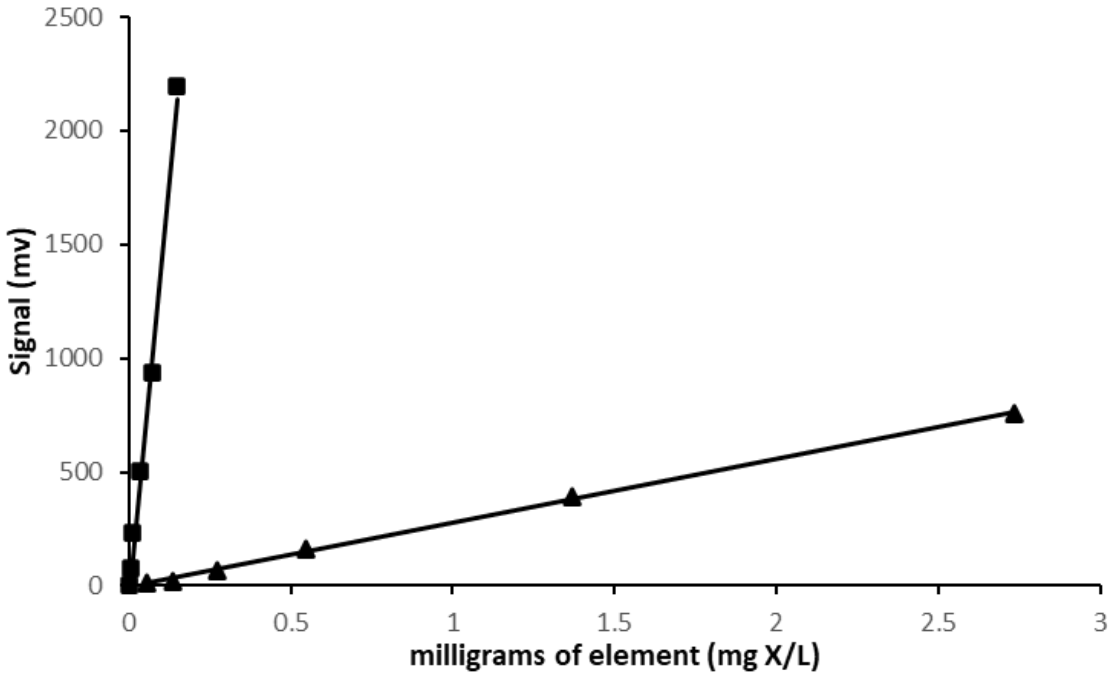

Figure 3-6: 6-point calibration plot of methane (▲) and diethylamine (■) in the AFID sensor. Gas flows were 40 mL/min air, 14.5 mL/min hydrogen.

This LOD for nitrogen is on the upper end of the low pg detection limits typically reported for the AFID but still falls on the same order as these values.[44] Regardless, this is quite a reasonable value considering the key operating differences here. For instance, GC-AFID delivers analyte to the detector by inert carrier gas added to the hydrogen flow entering the flame inner cone while air flows concentrically around it.[44] Conversely, as with many air sensors, analyte here is drawn into the device along with the supporting air flow into the flame outer cone, without inert gas diluting flame species or temperature. Thus, this could alter flame chemistry and lead to premature analyte oxidation and reduced response. Still, the value above is analytically useful as, for example, many nitrogen-bearing chemical warfare agents are lethal at ~10-100 ng N/s and thus require detection at and below this level.[11,60]

As illustrated in Figure 3-6, DEA shows a considerably enhanced response, whereas with methane, much less sensitivity is observed as the carbon signal changes relatively little over the concentration range investigated. This yields a selectivity for nitrogen response over carbon of about two orders of magnitude on a per gram of element basis (g N/g C), which is somewhat lower than expected from GC-AFID and is likely due to the differences in analyte introduction noted above.[44] Nonetheless, the sensor demonstrates a clear bias towards nitrogen compounds in analysis.

3.4.2 Linear Response

As seen in Figure 3-6, both organonitrogen and hydrocarbon compounds exhibit linear profiles over these low-end concentrations. Figure 3-7 again demonstrates this linear profile for both methane and DEA over three orders of magnitude. This is consistent with other reports of linearity in the AFID that range from three to six orders of magnitude. Generally, it is expected that these curves will extend to some degree at higher analyte concentrations before ultimately plateauing as the detector response becomes saturated, however, this could not be observed here. This is primarily due to analyte sample bag preparation, where the vapor pressure of DEA limited its ability to transfer to the gas-phase at higher amounts. Additionally, higher levels of methane could also not be achieved since high sample bag concentrations resulted in the flame extinguishing. Nevertheless, it is apparent that this sensor exhibits a linear profile for organonitrogen species as well as hydrocarbon-based species.

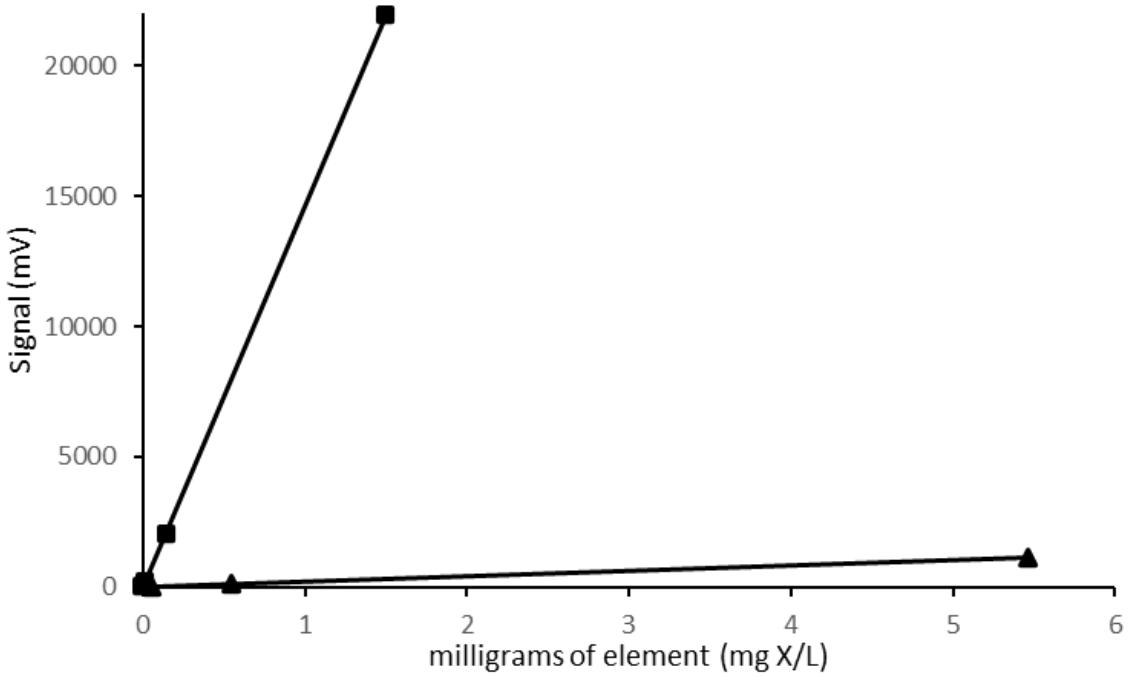

Figure 3-7: Calibration plot of the AFID sensor over three orders of concentration for both methane (▲) and diethylamine (■). Gas flows were 40 mL/min air, 14.5 mL/min hydrogen.

3.5 Response to Various Compounds

3.5.1 Response to Nitrogen Compounds

While the primary compounds used in determining detector optimums and traits were DEA and methane, impacts of molecular structure and chemical properties on sensor response remain to be studied. To test the response of other nitrogen compounds, 1 µL aliquots of some 12 different analytes were prepared in sample bags (~900 ng compound/mL) and examined with the AFID sensor. The response obtained for each (in mV/mol N) was then normalized for comparison with respect to the median value, assigned to propylamine. Typical results are shown in Table 3-1, where a wide range of nitrogen-containing analytes yield varying signal strength. Of note, with few exceptions, most respond much greater than methane, which is shown for comparison. For instance, most

alkylamines respond similarly regardless of carbon chain length or branching. While butylamine response is a bit smaller, this appears unrelated to its lower volatility, as trials with heated sample bags (60 °C) yielded no difference. Cyclic analytes also responded in similar fashion. Multifunctional analytes like ethylenediamine were also investigated, but the response was inconsistent and inconclusive due to their polarity and non-volatility.[42,56] Thus, the analyte structural differences above did not yield a major impact on response. Conversely, oxidized nitrogen compounds produced a dramatically lower response that was similar to methane. Ammonium hydroxide also gave similar results. These findings are reasonable since the underlying AFID response mechanism is largely believed to rely upon the analyte forming CN· radicals in the flame.[19,25,48,50] Thus, the inability of oxidized and inorganic nitrogen species to produce such species could lead to their low response, as noted previously.[48] This lack of sensitivity towards these species is considered a substantial asset. Given that the vast majority of atmospheric nitrogen is oxidized (NO_x) or inorganic (NH_3), the lack of response towards these species allows for airborne sampling of other agents without worry of background interferences due to these species.[7]

Table 3-1: AFID response toward various nitrogen compounds

Analyte	Relative Response*
butylamine	0.63
propylamine	1.00
ethylamine	1.00
diethylamine	1.14
triethylamine	1.31
isopropylamine	1.30
pyridine	0.73
pyrrolidine	0.99
piperidine	1.09
nitromethane	0.06
t-butyl nitrite	0.04
ammonium hydroxide	0.04
methane	0.01

* = mV/mol N response normalized to propylamine (median value); concentrations were ~ 900 ng/mL compound each

3.5.2 Response to Heteroatomic Compounds

As discussed, the AFID is sensitive to other heteroatoms in addition to nitrogen. The AFID sensor was examined with organic analytes containing oxygen, chlorine, sulfur and phosphorus. Similar to Table 3-1, Table 3-2 displays the typical results for such analytes with their response (in mV/mol element) normalized to DEA for comparison. As seen, oxygenated hydrocarbons responded weakly, like methane, indicating oxygen had no apparent impact on analyte response. By comparison, chlorine species also yielded a similar low-level signal, but it was instead negative, akin to other reports of organic halide response in the AFID.[42,55] This too suggests that chlorine, and likely other halogens, have little impact on analyte response. Conversely, trimethyl phosphite (TMP) produced a nearly 100-fold greater response than DEA. This is anticipated as the AFID is also conventionally

used for phosphorus detection, which is known to yield 100 times more sensitivity than nitrogen.[42,54] Surprisingly, carbon disulfide also elicited a relatively strong response that was about half of that obtained for diethylamine. This is interesting since the AFID typically yields weak and/or negative responses toward such analytes, although certain designs have reported positive sulfur sensitivity on par with nitrogen.[53,57]

Table 3-2: AFID response toward various heteroatomic organic compounds

Analyte	Relative Response*
diethylamine	1.00
methane	0.01
methanol	0.01
acetone	0.02
tetrahydrofuran	0.02
dichloromethane	-0.01
chloroform	-0.01
trimethyl phosphite	110.24
carbon disulfide	0.56

*= mV/mol element response normalized to diethylamine (N responder); concentrations were ~900 ng/mL compound each except for trimethyl phosphite and carbon disulfide at ~13 ng/mL

Also interesting is that the phosphorous and sulfur analytes above yielded highly asymmetric signals. For instance, sulfur signals consistently tailed greatly and took nearly an hour to return to baseline. Phosphorous behaved similarly at higher concentrations, but near 10 ng/mL or lower it reverted to a sharp symmetrical signal akin to that of nitrogen. It is unknown if this effect is specific to all such analytes, but if so, it could act as a further qualitative indicator of their presence since this was not observed for any other compounds.

Figure 3-8 illustrates the typical analyte signal profiles seen, where the characteristic noisy, tailing carbon disulfide signal (peak 10) is notable among them.

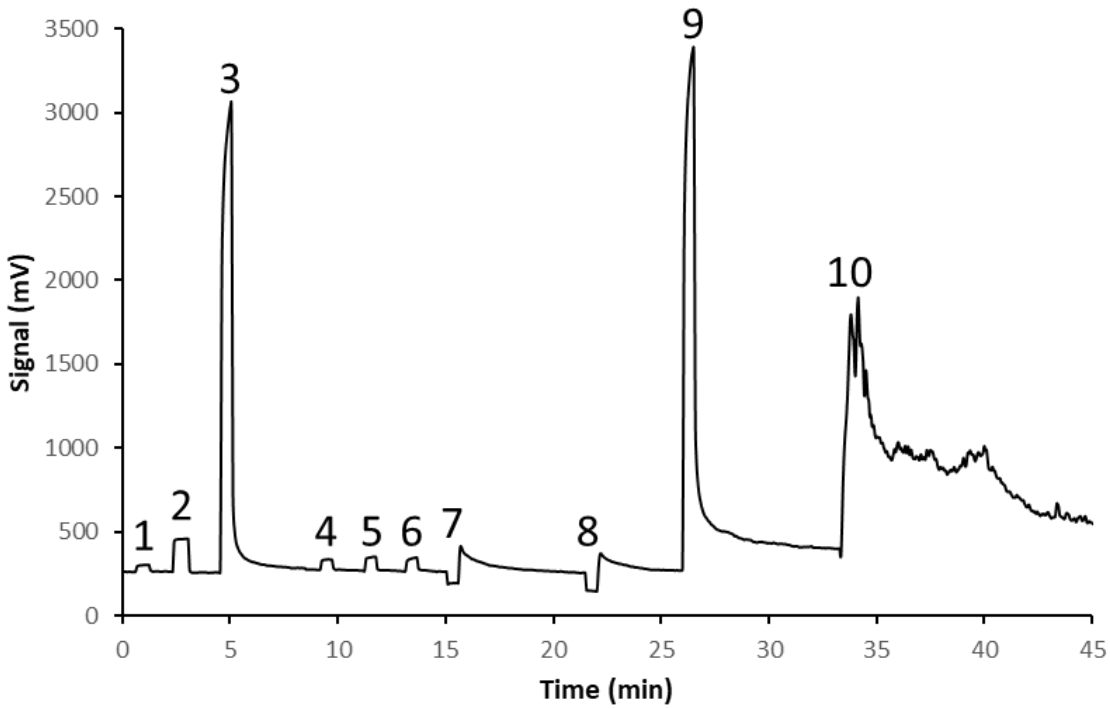

Figure 3-8: AFID sensor response toward various analytes under the optimum conditions. Analytes are: 1. air, 2. methane, 3. diethylamine, 4. methanol, 5. acetone, 6. tetrahydrofuran, 7. dichloromethane, 8. chloroform, 9. trimethyl phosphite, and 10. carbon disulfide. Concentrations are about 900 ng compound/mL each, except analytes 9 and 10 which were 12 and 140 ng/mL respectively.

An interesting phenomenon occurred when testing various heteroatomic compounds. After TMP was tested in large amounts (>1100 ng/mL), DEA signals seemed to increase in height. As shown in Figure 3-9, DEA signals more than doubled in height after the concentrated TMP peak had come through the system. However, noise also drastically increased in the system, overall decreasing S/N values. This occurrence has been seen in past TID systems, which showed that successive injections of 1 µL trimethyl

phosphate in 10 min led to an enhanced response for repeat injections.[48] The author suggested that this was a result of reactive species forming at the salt source, which led to enhanced degradation or ionization efficiencies. Though interesting, the practicality of this phenomenon is of no benefit at this time and was not further examined here.

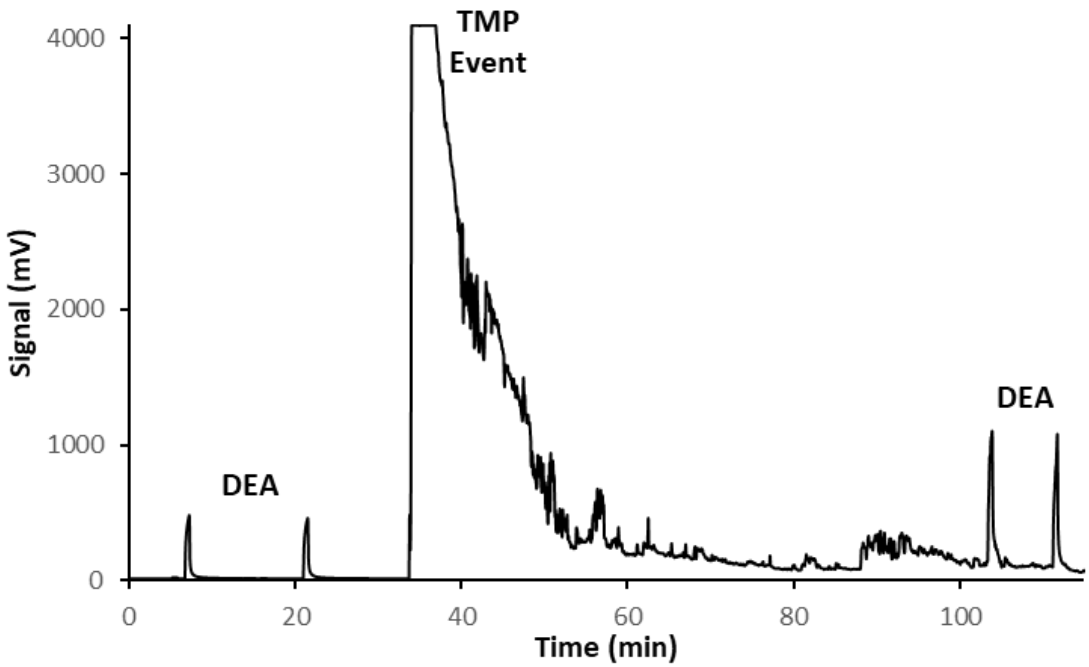

Figure 3-9: AFID sensor response to diethylamine sample bags (800 ng/mL) before (leftmost peaks) and after (rightmost peaks) sensor was subjected to concentrated levels of trimethyl phosphite (>1100 ng/mL) for ~30 seconds.

3.5.3 Response to Common Atmospheric Gases

In addition to specific analyte responses, other common atmospheric components such as nitrogen, carbon dioxide, and oxygen were explored with the sensor. Air bags were spiked with 10 mL aliquots of each gas and tested against a pure air bag. Both nitrogen and carbon dioxide bags exhibited a small signal decrease compared to the air bag, and as

additional aliquots were added, the signal response continued to fall. Conversely, the oxygen-spiked bag slightly increased in signal height. This indicates baseline response is primarily affected by the oxygen content of the sample. This is reasonable, given air is the primary oxidation source for the flame, and as the oxygen percentage of the intake air changes, so do flame properties like temperature and ionizing potential. Similarly, this is why the air bags demonstrate a slight positive peak, as they likely have a higher oxygen ratio than the ambient air.

Humidity was also briefly investigated by similarly spiking air bags with 10 µl of deionized water and letting it evaporate. Like nitrogen and carbon dioxide, the signal height was slightly decreased compared to the air bag, likely owing to oxygen displacement in the flame. The impact that altering oxygen and humidity sample matrix ratios have on analyte response remains to be examined in depth, but it is currently notable that none of the gases or the water vapor responded strongly or altered peak shape.

3.6 Conclusion

A novel AFID sensor was developed for the selective detection of airborne organonitrogen analytes. Here, several design variations were explored, and the reasoning for them explained, as well as the overall optimization and characterization of the device. Ultimately, a planar, four-channelled format constructed of quartz was adopted. This allowed for the inclusion of all components necessary for AFID detection mechanisms. Furthermore, this design was simple, lightweight, compact, and portable, all attractive features of a sensor-based detection system. The system was further characterized and

optimized by observing general traits of detection response and how signals were affected by several variables. Use of $RbSO_4$ as the alkali salt was found to provide the best signal response in addition to maintaining optimal contact between the salt and flame. Flame gas flows were found to be ideal at 40 mL/min of air and ~14.5 mL/min of hydrogen.

Once optimized, quantitative detector characteristics were inspected, producing figures of merit. The sensor showed obvious selectivity for organonitrogen species over purely organic species giving an LOD of 30 pg N/s and 2800 pg C/s and a selectivity of $\sim 10^2$ g C/g N. Additionally, signal response was found to correlate linearly with analyte concentration over three orders of magnitude.

Lastly, the signal response of various nitrogen-containing compounds, organic heteroatomic species, and common atmospheric components was studied. Some variances between organonitrogen species were noted, with inorganic and oxidized nitrogen compounds showing very little response in comparison. Oxygen- and chlorine-containing species responded minimally, like hydrocarbons, while phosphorus was ~100 times more selective than nitrogen. Sulfur also showed an unexpectedly high response (~0.5 times less selective than nitrogen), but its characteristic signal profile is expected to aid in its recognition. Finally, N_2, CO_2, and water vapor were all shown to displace oxygen in the flame, which can slightly affect baseline response.

Chapter Four: Selective AFID Sensor Detection and Tandem Detector Applications

4.1 Introduction

Having optimized and investigated the analytical parameters of the AFID sensor, a direct comparison to a conventional detector was initiated. As mentioned previously, the FPD has been used in several sensor-based detection systems, mainly for sulfur and phosphorus but has seen a limited use for nitrogen. It is also flame-based as well is similar in cost and complexity to the AFID. As such, the AFID sensor response was compared to that of a typical FPD to demonstrate its selectivity for nitrogen.

Furthermore, while the FPD is weak in its ability to identify organonitrogen compounds, it provides excellent information regarding other species like sulfur and phosphorus. To capitalize on this perception, the aforementioned sensors were coupled together as a means to gain more information about a sample in a single test. This also helps to limit false positives in the AFID and allows for detector-specific ratios, which can further be used as a general screening tool for specific elements. The use of this ratio, as well as its dependence on sample structure and concentration, will be examined as well.

Lastly, to evaluate the analytical utility of the standalone AFID sensor as well as the tandem AFID/FPD, both were employed in the analysis of several real-world samples. Applications include petrochemical and organic matrices, as well as chemical warfare simulant testing.

4.2 AFID and FPD Sensor Comparison

To achieve a direct comparison between detectors, a standard FPD was fitted with a gas-phase analyte introduction system like that used in the AFID. The PMT of the FPD was also fitted with a 240-395 nm band pass filter to better isolate the luminescence stemming from nitrogen in the flame and to minimize background interference.[39] From an architectural point of view, the construction of the AFID sensor is relatively simple compared to the FPD. For instance, aside from the weight and size differences of the employed FPD, it requires a light-tight housing as well as a PMT and light guide which adds cost and bulkiness when designing an FPD sensor. By contrast, the AFID sensor can be operated in open light and requires a single collector electrode. It must be noted that while both sensors employed the same analyte delivery system, the flow of the micro-air pump of either detector was slightly different, with the AFID pump flowing ~1.5 times greater than the FPD. However, the flows used are necessary as they provide optimal detection conditions in either sensor. Thus, this allows a direct comparison of sensor performance when faced with the same concentration of analyte.

To determine the N/C selectivity, methane and DEA sample bags were tested on each system individually. For the same concentration of DEA exposed to each sensor, the AFID produced 16.6 times larger signals (n=5) and ~10 times less noise, providing a two-order of magnitude increase (~160 times) to analyte S/N ratio compared to the FPD (Figure 4-1). The AFID sensor also produced a N/C response selectivity of 60.1, while in the FPD, the N/C selectivity was only 3.6, a ~1600% increase. This primarily stemmed from a much larger AFID nitrogen signal, as carbon response varied little between the devices. Even considering that the air pump analyte mass-flow of the FPD is slightly lower than that of

the AFID, the signals generated in the proposed sensor still offer superior selectivity and S/N values. Thus, these results are favorable for the AFID sensor and demonstrate the difficulty in analyzing for nitrogen with the FPD, as it typically provides a nitrogen response that is only marginally larger than that of carbon.

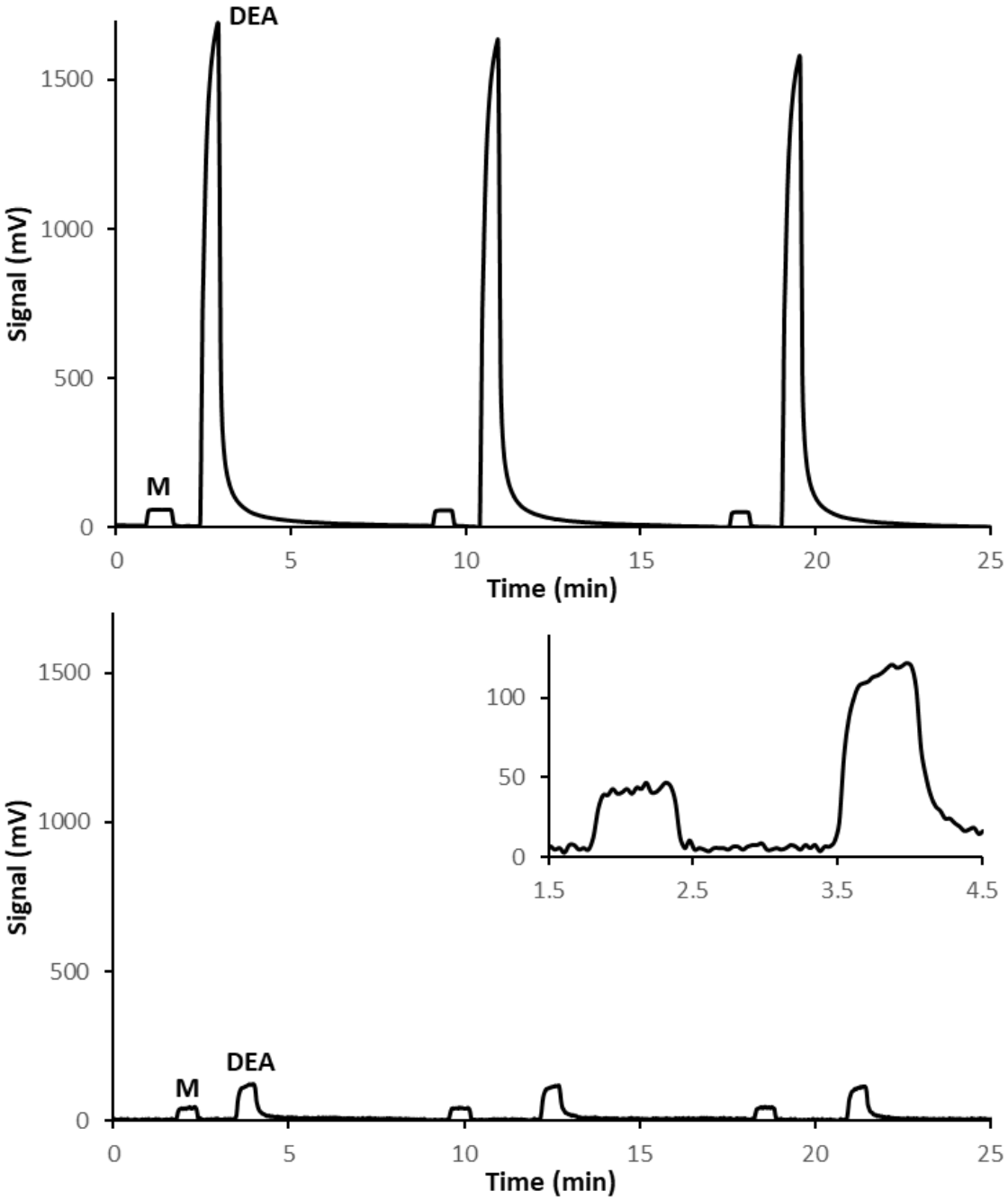

Figure 4-1: Comparison of identical methane (M) and diethylamine (DEA) sample signals in both the AFID (top) and FPD sensors (bottom). A magnified image of the first set of peaks in the FPD is also shown. Analyte concentrations are ~800 ng/mL each.

4.3 Tandem Detector System

4.3.1 Response Ratios

While the AFID sensor can offer improved performance, like all isolated detection methods, it remains subject to the difficulty in ultimately discerning target analytes from background hydrocarbons present. For instance, although the AFID and FPD each selectively detect nitrogen to different degrees, a lone signal from either sensor can lead to false determinations since it is difficult to ascertain if it arises from a target nitrogen analyte or an abundant hydrocarbon interferent. This is further problematic due to the absence of GC separation in these sensor modes and the qualitative information that is missing from analyte retention. To aid this, many modern sensor platforms, as well as traditional GC systems, have used multiple devices to detect a sample.[59,60,67] Even more useful is the combination of simultaneous signals from different detection modes to obtain a unique analytical signature for different species. For instance, this has been employed previously in GC separations, where the response ratio between the AFID and the FID,[68] or separate wavelength channels of an FPD,[39] has been used to gain structural and elemental composition information about an analyte. Since this approach has not been used for nitrogen detection in a dual AFID and FPD sensor without GC separation, it was investigated further here.

For this, the AFID and FPD sensors were connected in parallel such that a sole sample inlet led into a tee union that split the analyte flow into separate paths. In this way, the respective micro-air pump of each detector drew sample simultaneously and independently from the same source. An example of the data captured from this setup is shown in Figure 4-2. As seen in Figure 4-2A, the signals obtained from each device overlap

very well and display near-identical profiles. Strictly based on visual observation of these signals (and knowledge about the specificity of either detector), it is apparent that the first signal is likely hydrocarbon based as neither detector is selective towards carbon. Conversely, the second peak can be assumed to contain nitrogen as the AFID generates a large signal while the FPD does not. Similarly, if both the AFID and FPD were to yield an enhanced response, it could indicate that phosphorus is present. While this is simply an educated guess prone to incorrect assumptions and potentially false identification, it is a rapid method that provides qualitative information about the analyte.

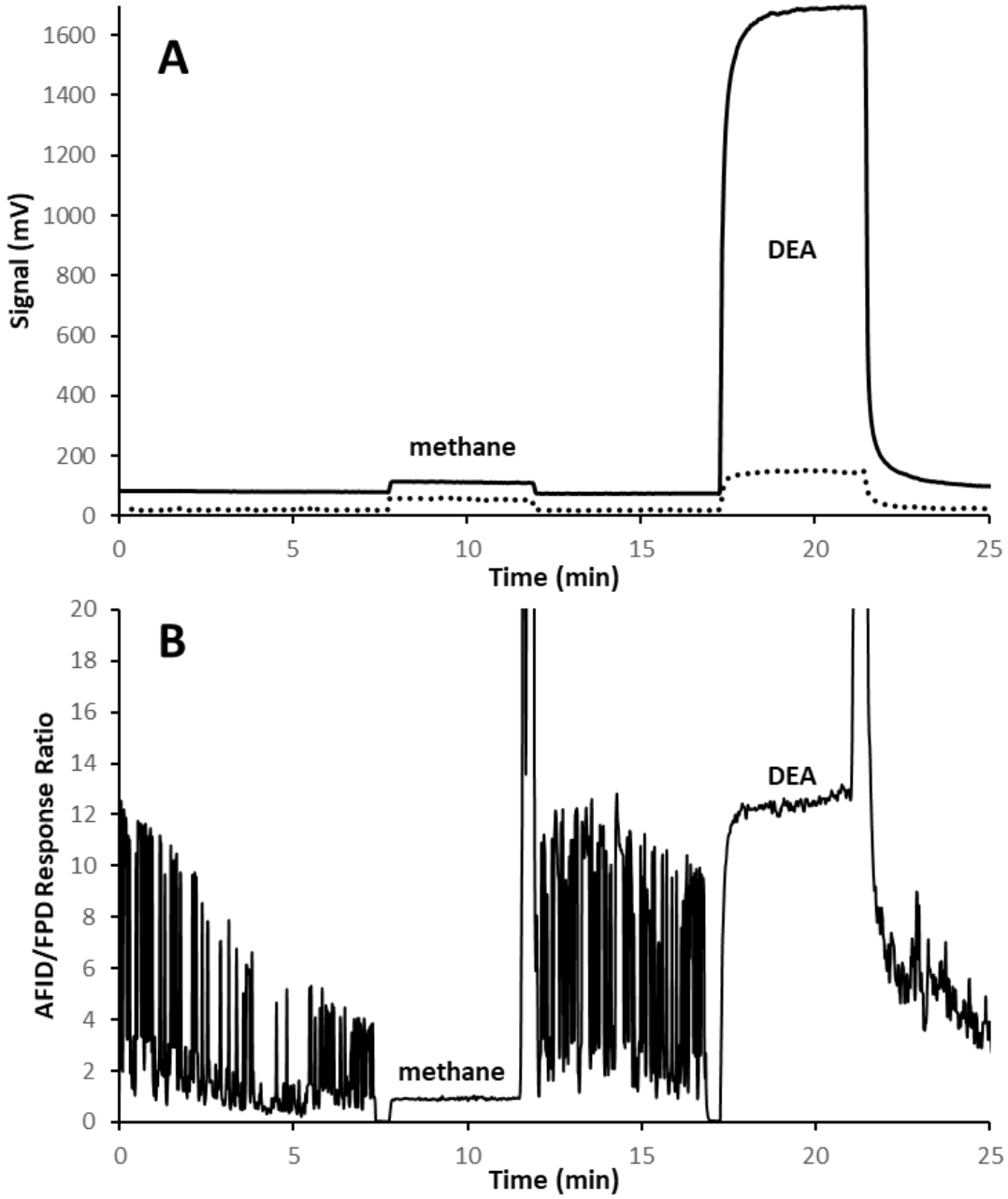

Figure 4-2: Simultaneous sensor response toward a methane and diethylamine (DEA) sample in both the AFID (solid line) and FPD (dashed line) devices under optimum conditions. Concentrations are about 800 ng/mL each. B) The ratio of the response traces shown in A after baseline subtraction.

Taking this a quantitative step further, a more powerful outcome is obtained when the ratio of these signals in either detector is acquired, as shown in Figure 4-2B. Here, specific to the analyte character and its response in each detector, the AFID/FPD ratio can be quantified, and for DEA is about 13 in this trial, while for methane it is near 1. As such, these distinct ratios can offer greater confirmation of analyte identity. Moreover, it can be seen in Figure 4-2B that the ratio of random background noise from each device yields high variability in the value obtained. However, when an analyte is present, the correlated signals from each sensor rapidly produce a more uniform and unique ratio. For instance, the ratio values obtained between the analyte signals (~12-17 minute range) varied by about 70 %RSD, whereas those obtained for carbon (~8-11 minute range) and nitrogen (~17-21 minute range) varied by only 2-4 %RSD. Thus, this information can also be used to potentially detect a chemical "event" through the onset of signal correlation, in addition to identifying the analyte present.

4.3.1.1 Concentration and Compound Dependence

While detector ratios offer an approach that can detect a chemical "event" and subsequently provide information about the atomic content of the chemical, it is unknown if this ratio is constant with changes in molecular structure and compound concentration. Table 4-1 shows the impact of analyte concentration on the average response ratio obtained for DEA and methane (n = 4).

Table 4-1: Detector response ratios as a function of analyte concentration

Analyte	Concentration (ng/mL)	AFID/FPD Response Ratio
diethylamine	15	13.98
	75	12.47
	150	12.32
	375	14.92
methane	273	0.78
	547	0.83
	1367	0.82

As seen, over the range investigated, the AFID/FPD ratio of the nitrogen analyte yields somewhat consistent values with an overall result of 13.4 ± 1.0, giving a %RSD of 8.1%. Methane behaved more uniformly, giving an overall ratio of 0.81 ± 0.02 (2.7 %RSD).

Table 4-2 examines this ratio as a function of analyte structure. Here, the values obtained for the various nitrogen analytes range between 9.5 and 12.5. Conversely, the hydrocarbons examined all yielded ratios less than 1, except for methanol, which responded nearer to 2. This suggests that the ratio obtained has no major dependence on analyte concentration and structure. As such, since nitrogen-containing species provide distinctly different ratios in this tandem sensor setup than do hydrocarbons, this approach could facilitate the clearer identification of unknown analytes. In the future it would be interesting to explore additional sensors to see if specific ratios could be used to identify multiple analytes.

Table 4-2: Detector response ratios for various nitrogen and carbon-containing analytes

Analyte	AFID/FPD Response Ratios
diethylamine	12.49
pyridine	9.55
propylamine	11.84
isopropylamine	10.01
methane	0.90
hexane	0.39
tetrahydrofuran	0.77
benzene	0.31
methanol	2.29

- concentration of each is ~900 ng/mL

4.4 Method Applications

4.4.1 Impact of Sample Matrix on Signal Response

As briefly discussed, a sample matrix can play a significant role in the efficacy of a detection method. Selective detectors are often used to eliminate these background interferences but can still lead to false positives and mischaracterization of a sample. Moreover, certain matrices can often mask or trap a desired analyte, leading to false negatives. Thus, it is necessary to characterize the AFID sensor response to analytes present in various mediums.

The first sample matrix concerns the emission of aliphatic amines, which are present in vehicle exhaust emissions and their fuel sources.[69] Since they can significantly impact atmospheric chemical processes, their analysis in such matrices is of great interest.[69] Figure 4-3 shows the AFID sensor response to a 5, 13, and 26 %v/v sample of car exhaust

spiked with 800 ng/mL of DEA. As seen, a very clear, stable, and strong signal is obtained that depreciates as the volume of car exhaust in the sample bag increases. Since blank trials without DEA showed very low signals of only about 2 mV for car exhaust (5%) alone, the dominant signals in Figure 4-3 can be directly ascribed to the presence of the amine in the sample. Similar to tests regarding other atmospheric gases, the reduction in signal height with exhaust volume is attributed to the displacement of oxygen in the flame. Given that car exhaust is largely composed of N_2, CO_2, and water vapor, this is understandable.[70] Regardless, this test indicates the proficiency of the sensor to selectively detect organonitrogen analytes in a polluted sample environment.

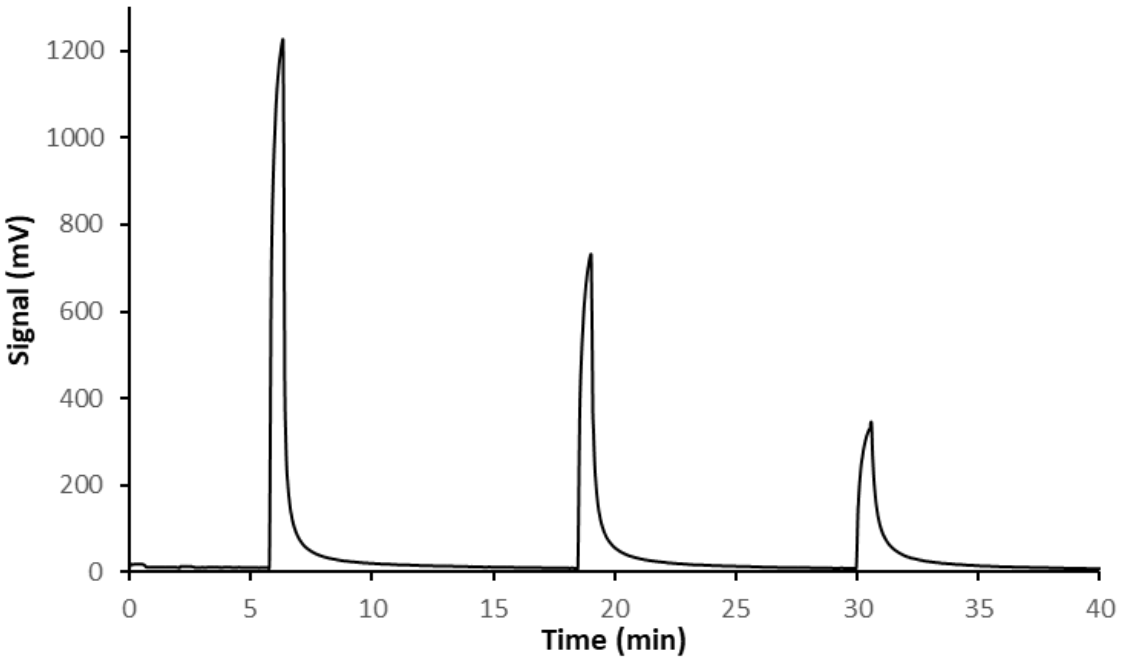

Figure 4-3: AFID sensor response to 5, 13, 26 %v/v of car exhaust to air sample bags (left to right) spiked with 800 ng/mL of DEA.

Likewise, petroleum matrices are of similar interest to car exhaust. Since field analysis is often hampered by the presence of other volatile substances, such as fuel vapor, this can lead to false positives. Therefore, samples of gasoline were prepared and spiked with DEA and tested in the tandem AFID/FPD system (Figure 4-4).

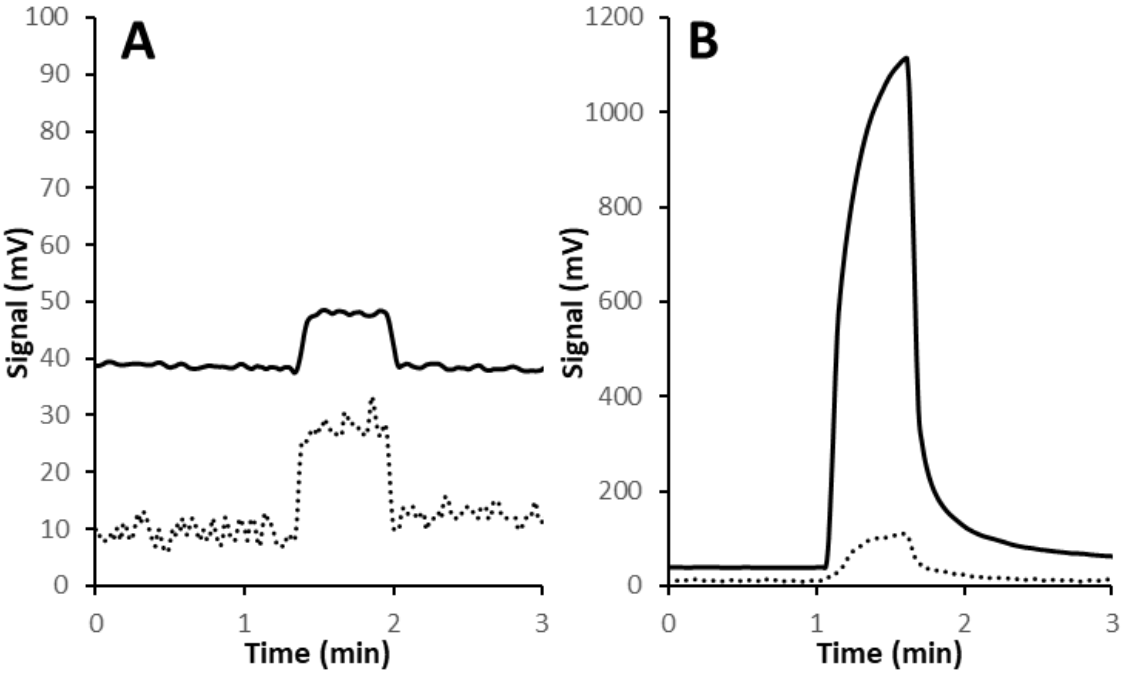

Figure 4-4: Simultaneous sensor response in both the AFID (solid line) and FPD (dashed line) devices to pure gasoline (A) and gasoline spiked with DEA (B). Concentrations are ~800 ppm of gasoline in either sample bag and 800 ng/mL of DEA in spiked bag.

Once again, based on the diminished AFID signal seen in Figure 4-4A, the enhanced signal in Figure 4-4B is directly due to the DEA present. Additionally, the AFID still exhibits excellent selectivity towards the target analyte in a polluted environment (Figure 4-4B) and does not show any degradation in signal due to the gasoline matrix when compared to a pure DEA sample bag (800 ng/mL). Furthermore, since inspection of this signal alone is unable to confirm the analyte identity, the AFID/FPD detector ratios were

calculated and showed values of 0.34 for pure gasoline and 11.8 for the spiked gasoline. This aligns with the findings above, where hydrocarbon compounds typically exhibited a ratio of <1 and nitrogen compounds averaged a ratio of ~13. Therefore, response ratios from tandem devices can help to ascertain analyte identity and prevent false positives.

More remotely, the noxious odor of certain amines in areas such as markets also prompts a related interest in monitoring for such species in fish and other natural sources.[71] Figure 4-5 shows the AFID sensor analysis of the headspace over a piece of fish containing DEA. Again, a clear, strong peak appears and is assigned to the analyte as the blank fish sample produced only a minor signal of about 4 mV. As well, since the DEA was present at a similar level as in Figures 4-3 and 4-4 (about 800 ng/mL), it is interesting to note that the smaller signal obtained in Figure 4-5 is likely due to the strong attraction of the fish tissue for the analyte versus the vapor phase.[71] This is corroborated by the observation that replicate signals of the same bag continued to diminish over roughly two hours until reaching only slightly higher levels to that of the unspiked fish response. Thus, certain sample matrices are shown to adsorb target analytes, which can limit but not eliminate response. This indicates the impact sample composition can have on the analyte, and in the future, it would be interesting to test the rate at which various sorbents are able to remove these analytes from an air sample. Nevertheless, such amines are shown they can be readily analyzed using the AFID sensor.

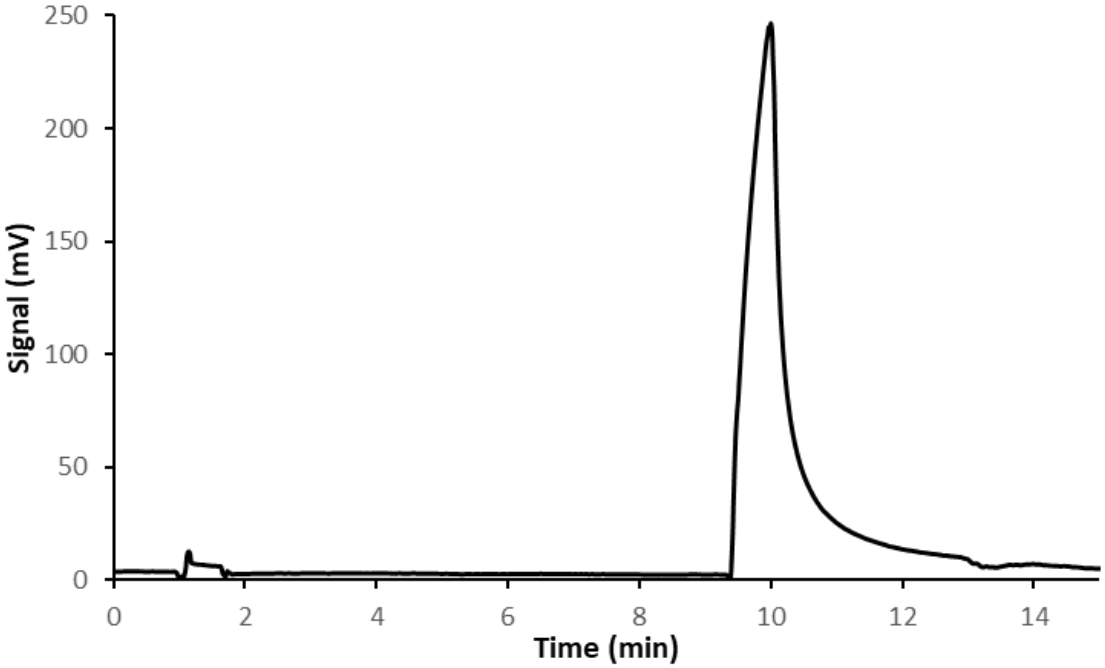

Figure 4-5*: AFID response to the headspace over a 10 g piece of dried fish meat without (left peak) and with (right peak) 800 ng/mL of DEA. Time from spiking to testing was ~10 min*.

4.4.2 Acetonitrile as a Chemical Warfare Surrogate

The second application concerned the analysis of acetonitrile (ACN), a toxin prominently present in biomass burning and which is also often used as a tracer in field research for the presence of similar cyanide related species.[72] Even more, the well-known chemical warfare agents cyanogen chloride (CK) and hydrogen cyanide (AC) hold similar properties to this analyte and is used in their production, making ACN a commonly employed surrogate for CK and AC in simulation testing.[73–75] Figure 4-6 shows the AFID sensor analysis of an air sample containing acetonitrile. As seen, it provides a very strong, well-defined signal for the analyte, which is present at 44 ng/mL. This concentration represents about half the equivalent amount of CK and AC believed to be immediately

dangerous to life or health (IDLH).[11,76,77] Thus, the AFID sensor could be appropriate for detecting such agents at low concentrations in threat assessment applications.[11,60,78]

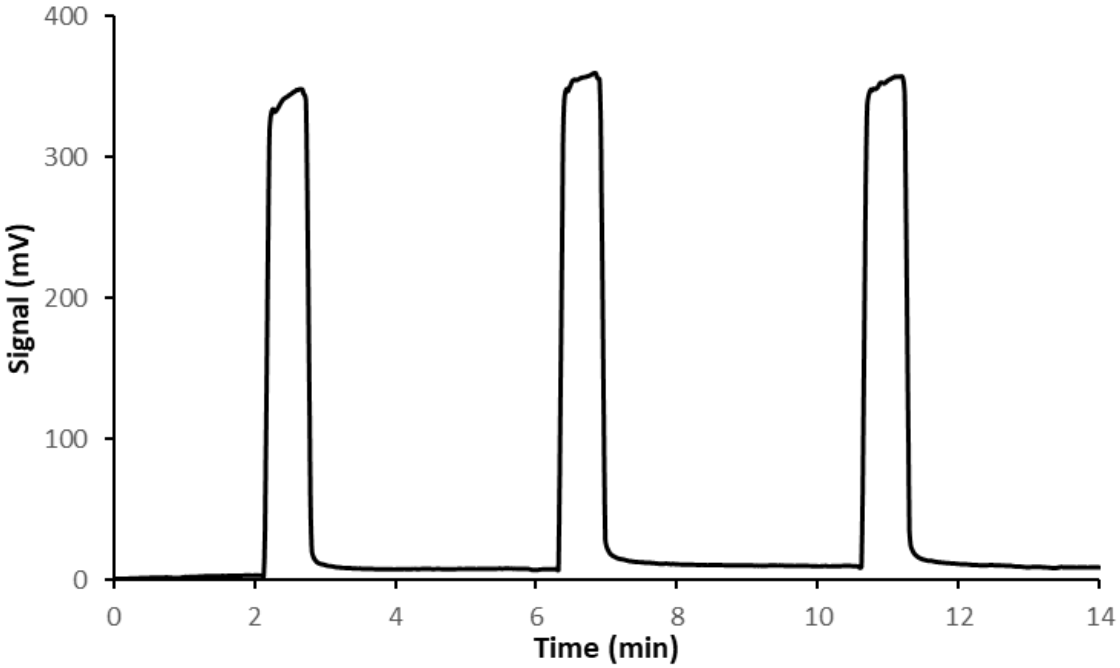

Figure 4-6: AFID sensor response to acetonitrile in air at a concentration equivalent to sub IDLH levels of CK/AC (44 ng/mL). Three replicate runs shown.

Further, ACN was also tested in the joint AFID/FPD sensor. It was found that ACN signals yielded a response ratio of ~17. While this is slightly higher than past ratios for nitrogen-containing species, it again demonstrates the difference in values between organonitrogen analytes and hydrocarbon-based matrices (e.g. gasoline). As such, the AFID sensor may be useful for analyzing volatile organonitrogen analytes in these and other applications.

4.5 Conclusion

The capabilities of the AFID sensor in terms of selectivity and sensitivity were compared to that of a typical FPD. The AFID was superior in N/C selectivity giving a ~16 times increase in both nitrogen response and N/C signal selectivity. Furthermore, the AFID could provide over a ~160 times increase in S/N values to that of the FPD under optimal detector conditions. This demonstrates the ability of the sensor to offer increased organonitrogen detection over conventionally used techniques. Moreover, the simplicity in design compared to an FPD offers additional benefits to such a system.

Aside from directly comparing the two systems, it was realized that using the FPD in tandem with the AFID offered the capability to gain additional knowledge about a sample. As such, the two detectors were placed in parallel to simultaneously detect a sample. From here, detector-specific ratios could be determined, which were found to be specific to the heteroatomic content of a sample. Further testing showed that this ratio is not significantly influenced by the concentration of the analyte nor the structure, as long as it contains the specific heteroatom necessary for response. This allows for a more detailed and precise molecular and structural determination of a sample, as well as facilitates the addition of other sensors and their subsequent ratios.

The applicability of the sensor, as an individual and in a tandem detection mode, was explored through the testing of various samples. The effect of interfering petrochemical and organic sample matrices were found to have little effect on target analyte response in the AFID. Even analytes in heavily polluted environments where oxygen in the flame was significantly limited produced a notable signal. However, sample matrices that

were able to adsorb analytes, like the fish, could reduce their availability in the gas-phase and limit, but not eliminate, signal response. Additionally, acetonitrile, a chemical warfare agent surrogate, was also able to be detected in sub IDLH levels which demonstrates the sensors use to aid in risk management. Detector ratios in the tandem detector setup were also analyzed and it was found that these ratios are consistent for target analytes in contaminated samples. Furthermore, real-world sample matrices produced similar ratios to that of laboratory standards.

Chapter Five: Summary and Future Work

5.1 Summary

The works detailed in this thesis explore the use of a novel AFID as a sensor for airborne organonitrogen compounds. Nitrogen-containing species are found in a variety of industries and are often toxic and can severely impact environmental conditions. Therefore, the identification and quantification of such species are important for regulatory and risk assessment measures. Unfortunately, currently available techniques for detection of these compounds are stationary in nature, making them unavailable for in-situ analysis. Portable detection methods do exist, however, they suffer from a lack of specificity or rely on complex detection mechanisms, which can make them complex and expensive. This work makes use of a lightweight, portable, inexpensive novel detection system to be able to selectively detect gas-phase organonitrogen compounds in the field.

The construction and general traits of the sensor were first explored to better understand conditions in which organonitrogen response was maximized. Detector design, flame gas flows, flame orientation, and alkali salt type and packing procedures were all found to influence signal response and, as such, were optimized to achieve the greatest signal enhancement for nitrogen species.

Once the signal response was optimized, characterization of the sensor was further examined. Specifically, it was found that signal response was largely uniform for various nitrogen-containing species, with the exception of inorganic and heavily oxidized species. The response to other heteroatoms was also examined, with oxygen- and chlorine-

containing compounds producing a minimal response akin to the hydrocarbons. The sensor demonstrated a selective response towards organophosphorus species as well with ~100 times selectivity over nitrogen. Sulfur also showed a higher response than expected but was often accompanied by a characteristic noisy, tailing response after it was sensed. Nitrogen, carbon dioxide, and water vapor were also shown to slightly impact baseline response and was likely due to the displacement of oxygen to the flame.

Next, the AFID sensor was compared to a commercially available flame-based sensor often used in similar applications. A conventional FPD was fitted with the same airborne analyte delivery system as the AFID and signals of both an organonitrogen and hydrocarbon were compared. It was found that the AFID provides over a 1600% increase in both nitrogen response and N/C selectivity. Additionally, noise was ~10 times smaller than the FPD, resulting in a ~160 times increase in S/N values. These two sensors were then coupled in parallel as a means to increase analyte identification by using qualitative analysis of signals from each detector. Additionally, by taking the signal ratio of the detector responses, quantitative values for compounds could be achieved. These values were found to be specific to heteroatom content, meaning this ratio could further aid in the identification of a sample.

Finally, the applicability of both the standalone AFID sensor as well as the tandem AFID/FPD system was examined using various sample matrices. First, the response of a target organonitrogen analyte in various sample matrices was examined. Ultimately, the sensor maintained a selective response in both petrochemical and organic sample matrices, although response intensity could vary depending on oxygen content as well as potential matrix-analyte binding processes over time. The sensor was also found to be able to detect

levels of acetonitrile, a surrogate for the blood agents CK and AC, that equate to sub IDLH levels for either compound.

Overall, this study illustrates the characterization and optimization of a novel detection system for in-situ analysis of compounds that currently require complex, expensive, and non-portable systems for analysis. This system can effectively provide a selective response for organonitrogens while minimizing background signals. Furthermore, coupling of this sensor allows for increased means of analyte identification and minimization of false positive signals.

5.2 Future Work

5.2.1 Detector Adaptions

As the sensor stands currently, it is able to respond selectively toward gas-phase organonitrogen species. Furthermore, coupling the AFID to another detector like the FPD was seen to help prevent false positive determinations. Continuing this trend and adapting the AFID/FPD tandem to multiple other detectors would provide even more information about a species. The FID is an easy add-on as this is just the proposed sensor without the alkali salt. Another simple change could be the use of several PMTs on an FPD with various filter combinations, each specific to a certain element (e.g. blue filter for sulfur, green filter for phosphorus). Research into developing these portable and cost-effective sensors remains a promising field, and as more of these systems are developed, it would be interesting to use many detectors in tandem for the identification of multiple analytes. Furthermore, as more detectors are implemented, detector response ratios between the pairs

of sensors could be monitored to build a more comprehensive identification profile of analytes.

Another adaptation could be the introduction of a separation column. This is the most obvious solution to discriminating sample matrices into their individual components. Several micro-GC columns have already been developed which would conform to both size and weight constrictions of the proposed sensor.[63,79] However, additional components like heating, potential carrier gases, and adapting the current sample inlet to work with one of these microcolumns are all issues that would need to be managed.

Until now, all samples tested were strictly gas-phase analytes (i.e. evaporated liquid analytes). However, not all airborne samples are present in the gas phase. For example, aerosols are a suspension of very fine liquid and/or solid particles in an air mixture. The relevance of this can be exhibited in applications such as pesticides (which are typically dispersed as liquid aerosols) or smoke from a burning chemical plant. It is unknown if the flame in the proposed sensor can properly break down and detect samples such as these. Therefore, a proposed solution is the use of a heating system at the sample inlet to concentrate and desorb these types of samples to the detector flame. For example, a small tube filled with an electrically heated mesh could be placed in front of the micro-air pump. As aerosolized samples come into contact with the heated metal, they could be vaporized to gas-phase fragments that might be easily detected in the flame. This system could also theoretically be used as a sample preconcentration technique, where the heated mesh is turned off, allowing for a build-up of sample on the mesh. The mesh could then be turned on, rapidly heating and “flashing off” the collected analyte. This would be beneficial for

trace analysis, where samples too low in concentration could be detected as they come through the sensor.

Aspirations for this device involve eventual field-testing of the device and, ultimately, in-situ analysis. Understandably, the device in its current form only includes essential components for detection. Future direction of the sensor includes adapting it into a handheld or drone-based system, where the device resembles a "black box." All components would be hidden within a single container and the only functional pieces are an on/off switch and a data readout. The AFID chip currently does not require any major changes to do this, however, electrical systems would need to be automated and minimized and a suitable housing to contain and protect all the sensor parts would need to be designed.

5.2.2 Applications

This thesis examined the ability of the AFID sensor to adequately detect organonitrogen species and demonstrated several real-world applications where it is beneficial to be able to sense these compounds. However, there are numerous industries where airborne organonitrogens are present and therefore are many additional applications that can be explored. As mentioned above, airborne analytes can also refer to ambient solid or liquid particulate matter. It is unknown how the detector is currently able to respond to these types of compounds. For instance, cigarette smoke contains many nitrogen-containing species[80], but unlike gaseous analytes tested in this research, the sample matrix is finely dispersed solid particles. Similarly, the use of fentanyl as a chemical warfare agent requires it to be disseminated as an aerosol either in its solid powder form or first dissolved

in a solvent.[11] It would be interesting to see how the AFID responds to some of these solid/liquid aerosols and how significantly signals vary in changes to the sample matrix.

Additionally, once the sensor is equipped for in-situ analysis, this opens the door to several air detection applications. Pipeline leaks, landfill and wastewater odor emissions, or chemical plant pollution are all applicable areas that require constant monitoring. A sensor could be placed in a static location to provide continuous detection in these areas. Similarly, this device could be placed on a drone to minimize human interaction in hazardous conditions and provide situational detection. For example, chemical transport spills and use of chemical warfare agents create hostile environments for human analysis. However, due to the portable nature of the sensor, it can be sent into these areas to assess risk levels and aid in recovery measures.

References

(1) Scully, F. E.; Hartman, A. C.; Rule, A.; LeBlanc, N. Disinfection Interference in Wastewaters by Natural Organic Nitrogen Compounds. *Environ. Sci. Technol.* **1996**, *30* (5), 1465–1471. https://doi.org/10.1021/es950375y.

(2) Rentsch, D.; Schmidt, S.; Tegeder, M. Transporters for Uptake and Allocation of Organic Nitrogen Compounds in Plants. *FEBS Lett.* **2007**, *581* (12), 2281–2289. https://doi.org/10.1016/j.febslet.2007.04.013.

(3) Akram, M.; Asif, H. M.; Uzair, M.; Akhtar, N.; Madni, A.; Shah, S. M. A. Amino Acids: A Review Article. *J. Med. Plants Res.* **2011**, *5* (17), 3997–4000.

(4) Vitaku, E.; Smith, D. T.; Njardarson, J. T. Analysis of the Structural Diversity, Substitution Patterns, and Frequency of Nitrogen Heterocycles among U.S. FDA Approved Pharmaceuticals: Miniperspective. *J. Med. Chem.* **2014**, *57* (24), 10257–10274. https://doi.org/10.1021/jm501100b.

(5) Prado, G. H. C.; Rao, Y.; de Klerk, A. Nitrogen Removal from Oil: A Review. *Energ. Fuel.* **2017**, *31* (1), 14–36. https://doi.org/10.1021/acs.energyfuels.6b02779.

(6) Taylor, O. C. Importance of Peroxyacetyl Nitrate (PAN) as a Phytotoxic Air Pollutant. *J. Air Pollut. Control Assoc.* **1969**, *19* (5), 347–351. https://doi.org/10.1080/00022470.1969.10466498.

(7) Jaffe, D. Nitrogen Cycle, Atmospheric. In *Encyclopedia of Physical Science and Technology*; Elsevier, 2003; pp 431–440. https://doi.org/10.1016/B0-12-227410-5/00922-4.

(8) Aktar, W.; Sengupta, D.; Chowdhury, A. Impact of Pesticides Use in Agriculture: Their Benefits and Hazards. *Interdisc. Toxicol.* **2009**, *2* (1), 1–12. https://doi.org/10.2478/v10102-009-0001-7.

(9) Risher, J., Choudhury, H., *Environmental Health Criteria 121: Aldicarb*; World Health Organization: Geneva, 1991. https://www.inchem.org/pages/ehc.html (accessed 2023-04)

(10) Ganesan, K.; Raza, S. K.; Vijayaraghavan, R. Chemical Warfare Agents. *J. Pharm. Bioallied Sci.* **2010**, *2* (3), 166–178. https://doi.org/10.4103/0975-7406.68498.

(11) Pacsial-Ong, E. J. Chemical Warfare Agent Detection a Review of Current Trends and Future Perspective. *Front. Biosci.* **2013**, *S5* (2), 516–543. https://doi.org/10.2741/S387.

(12) Caves, J. P. Fentanyl as a Chemical Weapon. In *CSWMD Proceedings 2019*, NDU Press: Washington, 2019.

(13) Berzas Nevado, J. J.; Villaseñor Llerena, M. J.; Contento Salcedo, A. M.; Nuevo, E. A. Determination of Fluoxetine, Fluvoxamine, and Clomipramine in Pharmaceutical Formulations by Capillary Gas Chromatography. *J. Chromatogr. Sci.* **2000**, *38* (5), 200–206. https://doi.org/10.1093/chromsci/38.5.200.

(14) Blomberg, J.; Schoenmakers, P. J.; Brinkman, U. A. T. Gas Chromatographic Methods for Oil Analysis. *J. Chromatogr. A.* **2002**, *972* (2), 137–173. https://doi.org/10.1016/S0021-9673(02)00995-0.

(15) Lehotay, S. J.; Hajšlová, J. Application of Gas Chromatography in Food Analysis. TrAC Trends Anal. Chem. 2002, 21 (9), 686–697. https://doi.org/10.1016/S0165-9936(02)00805-1.

(16) Hernández, F.; Portolés, T.; Pitarch, E.; López, F. J. Gas Chromatography Coupled to High-Resolution Time-of-Flight Mass Spectrometry to Analyze Trace-Level Organic Compounds in the Environment, Food Safety and Toxicology. *TrAC - Trends Anal. Chem.* **2011**, *30* (2), 388–400. https://doi.org/10.1016/j.trac.2010.11.007.

(17) Sampat, A.; Lopatka, M.; Sjerps, M.; Vivo-Truyols, G.; Schoenmakers, P.; van Asten, A. Forensic Potential of Comprehensive Two-Dimensional Gas Chromatography. *TrAC - Trends Anal. Chem.* **2016**, *80*, 345–363. https://doi.org/10.1016/j.trac.2015.10.011.

(18) Laski, R. R.; Watts, R. R. Gas Chromatography of Organonitrogen Pesticides, Using a Nitrogen-Specific Detection System. *J. Assoc. Off. Anal. Chem.* **1973**, *56* (2), 328–332. https://doi.org/10.1093/jaoac/56.2.328.

(19) Robards, K.; Ryan, D. *Principles and Practices of Modern Chromatographic Methods, 2nd ed.*; Academic Press, 2022.

(20) James, A. T.; Martin, A. J. P. Gas-Liquid Partition Chromatography: The Separation and Micro-Estimation of Volatile Fatty Acids from Formic Acid to Dodecanoic Acid. *Biochem. J.* **1952**, *50* (5), 679–690. https://doi.org/10.1042/bj0500679.

(21) Morey, T. E.; Booth, M. M.; Prather, R. A.; Nixon, S. J.; Boissoneault, J.; Melker, R. J.; Goldberger, B. A.; Wohltjen, H.; Dennis, D. M. Measurement of Ethanol in Gaseous Breath Using a Miniature Gas Chromatograph. *J. Anal. Toxicol.* **2011**, *35* (3), 134–142. https://doi.org/10.1093/anatox/35.3.134.

(22) Garg, A.; Akbar, M.; Vejerano, E.; Narayanan, S.; Nazhandali, L.; Marr, L. C.; Agah, M. Zebra GC: A Mini Gas Chromatography System for Trace-Level Determination of Hazardous Air Pollutants. *Sensor. Actuat. B-Chem.* **2015**, *212*, 145–154. https://doi.org/10.1016/j.snb.2014.12.136.

(23) Vitha, M. F. *Chromatography: Principles and Instrumentation*; John Wiley & Sons, Incorporated, 2016.

(24) Urban, P. L. Clarifying Misconceptions about Mass and Concentration Sensitivity. *J. Chem. Educ.* **2016**, *93* (6), 984–987. https://doi.org/10.1021/acs.jchemed.5b00986.

(25) Poole, C. F. Conventional Detectors for Gas Chromatography. In *Gas Chromatography, 2nd ed*; Elsevier, 2021; pp 343–369. https://doi.org/10.1016/B978-0-12-820675-1.00001-0.

(26) Harris C., D.; Lucy A., C. *Quantitative Chemical Analysis, 10th ed*; Macmillan Higher Education, 2020.

(27) Yan, X. Sulfur and Nitrogen Chemiluminescence Detection in Gas Chromatographic Analysis. *J. Chromatogr. A.* **2002**, *976* (1), 3–10. https://doi.org/10.1016/S0021-9673(02)01231-1.

(28) Burnett, C. H.; Adams, D. F.; Farwell, S. O. Relative FPD Responses for a Systematic Group of Sulfur-Containing Compounds. *J. Chromatogr. Sci.* **1978**, *16* (2), 68–73. https://doi.org/10.1093/chromsci/16.2.68.

(29) Farwell, S. O.; Barinaga, C. J. Sulfur-Selective Detection with the FPD: Current Enigmas, Practical Usage, and Future Directions. *J. Chromatogr. Sci.* **1986**, *24* (11), 483–494. https://doi.org/10.1093/chromsci/24.11.483.

(30) McWilliam, I. G.; Dewar, R. A. Flame Ionization Detector for Gas Chromatography. *Nature*. **1958**, *181* (4611), 760–760. https://doi.org/10.1038/181760a0.

(31) Harley, J.; Nel, W.; Pretorius, V. Flame Ionization Detector for Gas Chromatography. *Nature.* **1958**, *181* (4603), 177–178. https://doi.org/10.1038/181177a0.

(32) Poole, C. F. *The Essence of Chromatography*; Elsevier, 2003.

(33) Brody, S. S.; Chaney, J. E. Flame Photometric Detector: The Application of a Specific Detector for Phosphorus and for Sulfur Compounds - Sensitive to Subnanogram Quantities. *J. Chromatogr. Sci.* **1966**, *4* (2), 42–46. https://doi.org/10.1093/chromsci/4.2.42.

(34) Patterson, P. L.; Howe, R. L.; Abu-Shumays, Ahmad. A Dual-Flame Photometric Detector for Sulfur and Phosphorus Compounds in Gas Chromatograph Effluents. *Anal. Chem.* **1978**, *50* (2), 339–344. https://doi.org/10.1021/ac50024a042.

(35) Jing, H.; Amirav, A. Pulsed Flame Photometric Detector – a Step Forward towards Universal Heteroatom Selective Detection. *J. Chromatogr. A.* **1998**, *805* (1), 177–215. https://doi.org/10.1016/S0021-9673(97)01306-X.

(36) Clark, A. G.; Thurbide, K. B. An Improved Multiple Flame Photometric Detector for Gas Chromatography. *J. Chromatogr. A.* **2015**, *1421*, 154–161. https://doi.org/10.1016/j.chroma.2015.04.007.

(37) Aue, W. A.; Millier, Brian.; Sun, X. Yun. Elemental Specificity in Dual-Channel Flame Photometric Detection of Gas Chromatographic Peaks. *Anal. Chem.* **1991**, *63* (24), 2951–2955. https://doi.org/10.1021/ac00024a027.

(38) Aue, W. A.; Millier, B.; Sun, X.-Y. Flame Photometric Detection of Some Transition Metals. II. Enhancement of Selectivity. *Can. J. Chem.* **1992**, *70* (4), 1143–1155. https://doi.org/10.1139/v92-150.

(39) Aue, W. A.; Sun, X.-Y.; Millier, B. Inter-Elemental Selectivity, Spectra and Computer-Generated Specificity of Some Main-Group Elements in the Flame Photometric Detector. *J. Chromatogr. A.* **1992**, *606* (1), 73–86. https://doi.org/10.1016/0021-9673(92)85259-V.

(40) Giuffrida, L. A Flame Ionization Detector Highly Selective and Sensitive to Phosphorus—A Sodium Thermionic Detector. *J. AOAC Int.* **1964**, *47* (2), 293–300. https://doi.org/10.1093/jaoac/47.2.293.

(41) Giuffrida, L.; Ives, F. Investigation of Two Gas Chromatographic Techniques for the Determination of Organophosphate Pesticide Residues. *J. AOAC Int.* **1964**, *47* (6), 1112–1116. https://doi.org/10.1093/jaoac/47.6.1112.

(42) Ives, N. F.; Giuffrida, L. Investigation of Thermionic Detector Response for the Gas Chromatography of P, N, As, and CI Organic Compounds. *J. AOAC Int.* **1967**, *50* (1), 1–4. https://doi.org/10.1093/jaoac/50.1.1.

(43) Aue, W. A.; Gehrke, C. W.; Tindle, R. C.; Stalling, D. L.; Ruyle, C. D. Application of the Alkali-Flame Detector to Nitrogen Containing Compounds. *J. Chromatogr. Sci.* **1967**, *5* (7), 381–382. https://doi.org/10.1093/chromsci/5.7.381.

(44) Hartmann, C. H. Alkali Flame Detector for Organic Nitrogen Compounds. *J. Chromatogr. Sci.* **1969**, *7* (3), 163–167. https://doi.org/10.1093/chromsci/7.3.163.

(45) Karman, Arthur.; Haut, Harold. Alkali Flame Ionization Detector Attachment for Conventional Hydrogen Flame Ionization Detectors. *Anal. Chem.* **1973**, *45* (4), 822–824. https://doi.org/10.1021/ac60326a017.

(46) Greenhalgh, R.; Müller, J.; Aue, W. A. A Pure Rubidium/Quartz Source for Alkali Flame Ionization Detectors. *J. Chromatogr. Sci.* **1978**, *16* (1), 8–11. https://doi.org/10.1093/chromsci/16.1.8.

(47) Conte, E. D.; Barry, E. F. The Performance of a Dual Alkali Aerosol Flame Ionization Detector for Gas Chromatography. *Anal. Lett.* **1993**, *26* (12), 2711–2727. https://doi.org/10.1080/00032719308017987.

(48) Bombick, D. D.; Allison, J. Investigations Into the Response Mechanism of the Gas Chromatographic Thermionic Ionization Detector Part I. Mass Spectral Studies. *J. Chromatogr. Sci.* **1989**, *27* (10), 612–619. https://doi.org/10.1093/chromsci/27.10.612.

(49) Carlsson, H.; Robertsson, G.; Colmsjö, A. Response Mechanisms of Thermionic Detectors with Enhanced Nitrogen Selectivity. *Anal. Chem.* **2001**, *73* (23), 5698–5703. https://doi.org/10.1021/ac010204d.

(50) Kolb, B.; Bischoff, J. A New Design of a Thermionic Nitrogen and Phosphorus Detector for GC. *J. Chromatogr. Sci.* **1974**, *12* (11), 625–629. https://doi.org/10.1093/chromsci/12.11.625.

(51) Olah, K.; Szoke, A.; Vajta, Z. On the Mechanism of Kolb's N-P Selective Detector. *J. Chromatogr. Sci.* **1979**, *17* (9), 497–502. https://doi.org/10.1093/chromsci/17.9.497.

(52) McMahon, A. W.; Schofield, P. A. Probing the Response Mechanism of the Thermionic Detector by Resonance Enhanced Ionization Spectroscopy; Manchester, *AIP Conf. Proc.* **1998**, *454*, 301–304. https://doi.org/10.1063/1.57164.

(53) Dressler, M.; Janák, J. Detection of Sulphur Compounds with an Alkali Flame Ionization Detector. *J. Chromatogr. Sci.* **1969**, *7* (7), 451–452. https://doi.org/10.1093/chromsci/7.7.451.

(54) Brazhnikov, V. V.; Gur'Ev, M. V.; Sakodynsky, K. I. Thermionic Detectors in Gas Chromatography. *Chromatogr. Rev.* **1970**, *12*, 1-41.

(55) Gerhardt, K. O.; Aue, W. A. The Negative Alkali Flame Detector Response. *J. Chromatogr. A.* **1970**, *52*, 47–62. https://doi.org/10.1016/S0021-9673(01)96543-4.

(56) Aue, W. A.; Gerhardt, K. O.; Lakota, S. Determination of Hetero-Element Content in Organics by Alkali Flame—Gas—Liquid Chromatography. *J. Chromatogr. A.* **1971**, *63*, 237–249. https://doi.org/10.1016/S0021-9673(01)85636-3.

(57) Hoodless, R. A.; Sargent, M.; Treble, R. D. Communication. Sulphur Response of the Alkali Flame-Ionisation Detector. *Analyst*. **1976**, *101* (1206), 757–758. https://doi.org/10.1039/AN9760100757.

(58) Gao, L.; Song, Q.; Patterson, G. E.; Cooks, R. G.; Ouyang, Z. Handheld Rectilinear Ion Trap Mass Spectrometer. *Anal. Chem.* **2006**, *78* (17), 5994–6002. https://doi.org/10.1021/ac061144k.

(59) Ho, C.; Itamura, M.; Kelley, M.; Hughes, R. *Review of Chemical Sensors for In-Situ Monitoring of Volatile Contaminants*; SAND2001-0643; Sandia National Laboratories: Albuquerque, NM, 2001. https://doi.org/10.2172/780299.

(60) Sferopoulos, R. *A Review of Chemical Warfare Agent (CWA) Detector Technologies and Commercial-Off-The-Shelf Items*; Australian Department of Defense, Human Protection and Performance Division, Defence Science and Technology Organisation (DSTO): Victoria, 2008.

(61) Hayward, T. C.; Thurbide, K. B. Characteristics of Sulfur Response in a Micro-Flame Photometric Detector. *J. Chromatogr. A.* **2006**, *1105* (1–2), 66–70. https://doi.org/10.1016/j.chroma.2005.09.031.

(62) Hayward, T. C.; Thurbide, K. B. Novel On-Column and Inverted Operating Modes of a Microcounter-Current Flame Ionization Detector. *J. Chromatogr. A.* **2008**, *1200* (1), 2–7. https://doi.org/10.1016/j.chroma.2008.02.053.

(63) McKelvie, K. H.; Thurbide, K. B. Micro-Flame Photometric Detection in Miniature Gas Chromatography on a Titanium Tile. *Chromatographia*. **2019**, *82* (6), 935–942. https://doi.org/10.1007/s10337-019-03723-y.

(64) Karmen, A. Specific Detection of Halogens and Phosphorus by Flame Ionization. *Anal. Chem.* **1964**, *36* (8), 1416–1421. https://doi.org/10.1021/ac60214a007.

(65) Thurbide, K. B.; Anderson, C. D. Flame Photometric Detection inside of a Capillary Gas Chromatography Column. *Analyst.* **2003**, *128* (6), 616. https://doi.org/10.1039/b212727j.

(66) Thurbide, K. B.; Hayward, T. C. Improved Micro-Flame Detection Method for Gas Chromatography. *Anal. Chim. Acta.* **2004**, *519* (1), 121–128. https://doi.org/10.1016/j.aca.2004.05.047.

(67) Wessel, J. R. Collaborative Study of a Method for Multiple Organophosphorus Pesticide Residues in Nonfatty Foods. *J. AOAC Int.* **1967**, *50* (2), 430–439. https://doi.org/10.1093/jaoac/50.2.430.

(68) Baker, J. K. Identification and Chemical Classification of Drugs Based on the Relative Response of a Nitrogen Selective Detector and a Flame Ionization Detector in Gas Chromatographic Analysis. *Anal. Chem.* **1977**, *49* (7), 906–908. https://doi.org/10.1021/ac50015a009.

(69) Yang, D.; Zhu, S.; Ma, Y.; Zhou, L.; Zheng, F.; Wang, L.; Jiang, J.; Zheng, J. Emissions of Ammonia and Other Nitrogen-Containing Volatile Organic Compounds from Motor Vehicles under Low-Speed Driving Conditions. *Environ. Sci. Technol.* **2022**, *56* (9), 5440–5447. https://doi.org/10.1021/acs.est.2c00555.

(70) *Diesel and Gasoline Engine Exhausts and Some Nitroarenes*; International Agency for Research on Cancer, 1989.

(71) Moliner-Martínez, Y.; Campíns-Falcó, P.; Herráez-Hernández, R. A Method for the Determination of Dimethylamine in Air by Collection on Solid Support Sorbent with Subsequent Derivatization and Spectrophotometric Analysis. *J. Chromatogr. A.* **2004**, *1059* (1), 17–24. https://doi.org/10.1016/j.chroma.2004.10.021.

(72) Coggon, M. M.; Veres, P. R.; Yuan, B.; Koss, A.; Warneke, C.; Gilman, J. B.; Lerner, B. M.; Peischl, J.; Aikin, K. C.; Stockwell, C. E.; Hatch, L. E.; Ryerson, T. B.; Roberts, J. M.; Yokelson, R. J.; de Gouw, J. A. Emissions of Nitrogen-Containing Organic Compounds from the Burning of Herbaceous and Arboraceous Biomass: Fuel Composition Dependence and the Variability of Commonly Used Nitrile Tracers. *Geophys. Res. Lett.* **2016**, *43* (18), 9903–9912. https://doi.org/10.1002/2016GL070562.

(73) Hashimoto, K.; Morimoto, K.; Dobson, S. Enivironmental Health Criteria 154: Acetonitrile; World Health Organization: Geneva, 1993. https://www.inchem.org/pages/ehc.html (accessed 2023-04)

(74) Bigiani, L.; Zappa, D.; Barreca, D.; Gasparotto, A.; Sada, C.; Tabacchi, G.; Fois, E.; Comini, E.; Maccato, C. Sensing Nitrogen Mustard Gas Simulant at the ppb Scale via Selective Dual-Site Activation at Au/Mn_3O_4 Interfaces. *ACS Appl. Mater. Inter*. **2019**, *11* (26), 23692–23700. https://doi.org/10.1021/acsami.9b04875.

(75) Maccato, C.; Bigiani, L.; Carraro, G.; Gasparotto, A.; Sada, C.; Comini, E.; Barreca, D. Toward the Detection of Poisonous Chemicals and Warfare Agents by Functional Mn_3O_4 Nanosystems. *ACS Appl. Mater. Inter*. **2018**, *10* (15), 12305–12310. https://doi.org/10.1021/acsami.8b01835.

(76) United States Environmental Protection Agency. *Technical Support Document EPA/690/R-12/009F Provisional Peer-Reviewed Toxicity Values for Cyanogen Bromide (CASRN 506-68-3)*, National Center for Environmental Assessment Office of Research and Development: Cincinnati, OH, 2012.

(77) Ludwig, H. R.; Cairelli, S. G.; Whalen, J. J. *Documentation for Immediately Dangerous to Life or Health Concentrations (IDLHs)*; NTIS Publication No. PB-94-195047; U.S. Department of Health and Human Services: Cincinnati, OH, 1994. https://www.cdc.gov/niosh/idlh/pdfs/1994-IDLH-ValuesBackgroundDocs.pdf (accessed 2023-04).

(78) Ellison, D. H. *Emergency Action for Chemical and Biological Warfare Agents, 2nd ed*.; CRC Press, 2017. https://doi.org/10.1201/b19083.

(79) Regmi, B. P.; Agah, M. Micro Gas Chromatography: An Overview of Critical Components and Their Integration. *Anal. Chem.* **2018**, *90* (22), 13133–13150. https://doi.org/10.1021/acs.analchem.8b01461.

(80) Rodgman, A.; Smith, C. J.; Perfetti, T. A. The Composition of Cigarette Smoke: A Retrospective, with Emphasis on Polycyclic Components. *Hum. Exp. Toxicol.* **2000**, *19* (10), 573–595. https://doi.org/10.1191/096032700701546514.